ABSTRACT

Title of Thesis: MODEL COMPOUNDS GUIDE AFFINITY MEASUREMENT OF BERYLLIUM AND CALCIUM INTERACTIONS WITH PHOSPHOLIPIDS

Omid Davoudi, Master of Science, 2023

Thesis directed by: Professor Jeffery B. Klauda, Chemical and Biomolecular Engineering Department

Divalent cations bound to anionic lipids are necessary co-factors for many signaling mechanisms taking place at both the inner and outer surfaces of the cytoplasmic membrane. Coordination of divalent ions jointly by phospholipid headgroups and specific protein domains mediates recognition and triggers secondary messenger cascades or membrane fusion events.

Phosphoryl oxygens of phospholipids are common contributors to divalent ion coordination. With the aims of elucidating the affinities of the calcium ion (Ca^{2+}) and its toxic competitor beryllium (Be^{2+}) to different types of phosphate groups taking place in many 'building blocks' of the cell, improving simulation force fields and better understanding the nature of beryllium toxicity, here we use isothermal titration calorimetry (ITC) to study the thermodynamic parameters and coordination of these ions by phosphates. Particularly, we focus on the differences between phosphates in the phosphodiester configuration that connect the glycerol backbone with a headgroup (as in phosphatidylglycerol, PG) and terminal monoester phosphates such as in phosphatidic acid (PA) and most phosphorylated proteins. The comparison of small model compounds, dimethyl phosphate (DMP, mimicking phosphate in phosphatidyl glycerol) with glycerol-3-phosphate (Gly3P, emulating phosphate in phosphatidic acid) shows that the affinity of Be^{2+} for Gly3P is about one order of magnitude higher than for DMP and may exhibit at least two binding configurations. The Be^{2+} -DMP thermograms in most cases are well fitted with a one-site model. Upon completing the survey of small (model) compounds, we performed experiments to compare the binding parameters of Be^{2+} to POPA and to POPG-containing liposomes with the parameters obtained on respective model compounds. We also present several pilot binding experiments performed with POPS liposomes*;* however, the fit is poor.

MODEL COMPOUNDS GUIDE AFFINITY MEASUREMENT OF BERYLLIUM AND CALCIUM INTERACTIONS WITH PHOSPHOLIPIDS

by

Omid Davoudi

Thesis submitted to the Faculty of the Graduate School of the
University of Maryland, College Park, in partial fulfillment
of the requirements for the degree of
Master of Science
2023

Advisory Committee:
Professor Jeffery B. Klauda, Chair
Professor Sergei Sukharev
Professor Srinivasa R. Raghavan
Professor Ganesh Sriram

© Copyright by

Omid Davoudi

2023

Dedication

This thesis has been done with unconditional emotional support from my parents and without their enormous love there would be no inspiration to finish this thesis.

Table of Contents

List of Tables

List of Figures

List of Abbreviations

DLS	Dynamics Light Scattering
DMP	Dimethyl Phosphate
Gly3P	Glycerol 3- Phosphate
ITC	Isothermal Titration Calorimetry
MD	Molecular Dynamics
POPA	1-Palmitoyl-2-Oleoyl-sn-glycero-3-Phosphate
POPC	1-Palmitoyl-2-Oleoyl-sn-glycero-1-Phosphocholine
POPG	1-Palmitoyl-2-Oleoyl-sn-glycero-3-Phospho (1′-rac-glycerol)
POPS	1-Palmitoyl-2-Oleoyl-sn-glycero-Phospho-L-serine

Chapter 1: Introduction

Beryllium, being both light weight and hard, is a highly valuable non-magnetic metal that has been widely used for several decades in different manufacturing industries such as aerospace and sports industry as well as in nuclear reactors[1]. Soon after the start of extensive mining and manufacturing in the 1950's, it was discovered that this metal is toxic and frequently induces autoimmune response (berylliosis) in workers primarily dealing with beryllium dust[2]. The mechanism of toxicity was partially unraveled by characterizing a mutation in MHCII protein that abnormally coordinates beryllium ions, but the breadth of phenomenology of berylliosis, especially loss of macrophage function in contaminated tissues is still not completely understood. Recently, some data on the mechanism of competition between calcium (Ca^{2+}) and beryllium (Be^{2+}) ions for binding moieties on membranes' surfaces has been reported[3]. Further experimental and computational studies are needed to explain this binding more specifically for different membrane compositions. The thermodynamics binding of divalent ions to phosphodiester and phosphomonoester oxygens is highly significance for both lipids and phosphorylated proteins. Competitive binding of divalent ions and specificity of coordination by nucleotides and nucleic acids presents another chapter of biomedical science[4]. Binding of divalent ions to lipid vesicles is important for our understanding of relevant physiological processes such as signaling inside and outside of the cell, exocytosis, synaptic transmission, cell fusion and locomotion. However, the inaccurate description of ions parameters in Molecular

Dynamics (MD) Simulations impose limitations to study ion-lipid interactions by this computational method in atomistic details. Here, we aim to compare different binding modes with experimental results to get a better picture of interactions between negatively charged liposomes and positive divalent ions of calcium and beryllium, which should lay grounds for the forcefield refinement in the near future. Undoubtedly, computational methods augment and complement experimental results, and several studies have been set to compare experimental data on ion binding to phospholipids with the results of simulations[5].

Association of inorganic ions with phospholipids can occur in multiple configurations, which frequently induces a number of different conformations of headgroups, condenses lipids and changes lipid hydration (water displacement). When observed calorimetrically, the net heat and entropy can be obtained with good accuracy and suggest the driving forces, affinity, and some information on binding configurations. On the other hand, the same conformations could be sampled by MD simulations and compared directly with binding stoichiometry derived from Isothermal Titrations Calorimetry (ITC) (more details on ITC interpretation will be given in Methods section). For instance, Knecht et al [6] has reported 1-Palmitoyl-2-Oleoyl-sn-glycero-1-Phosphocholine (POPC) binding affinities obtained in ITC experiments with Na^+ and K^+ ions for different forcefields. Apparent binding constants for both ions were in good agreement with ITC experiments, however none of the forcefields could successfully reproduce both intrinsic and apparent binding constants simultaneously. They argued that this result stems from the fact that POPC carries negative charge at pH=7 based on electrophoresis experiment, however POPC

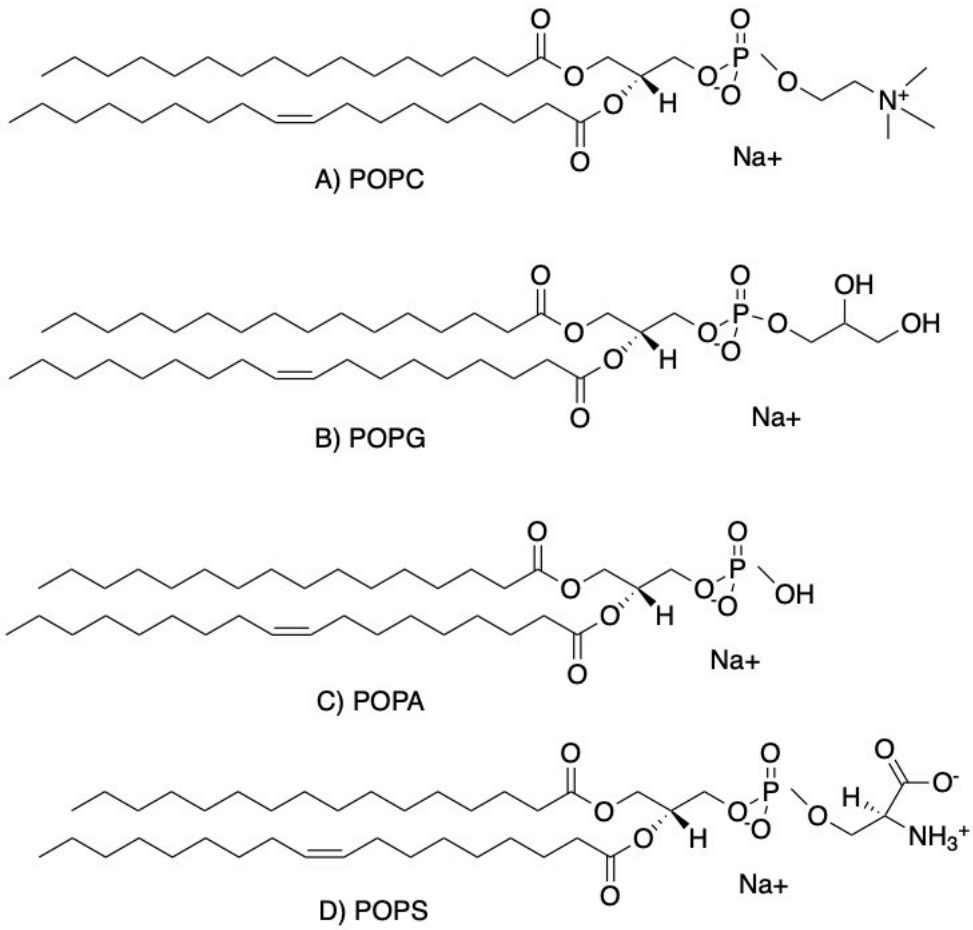

Figure 1. Lipid structures used in this study by CHEMDRAW

should be neutral in pH=7 (which is true in MD simulation). The difference between apparent and intrinsic binding constants have been defined based on ion concentrations in the bulk (for apparent) and ion concentrations near the lipid surface using electrophoretic mobility and Gouy-Chapman theory. However, this study focuses solely on the binding constants. In other words, the binding conformations have been considered as one to one binding stoichiometry at 500 mM concentration of ions despite the fact that ion-lipid association from experiments shows mixing stoichiometry[7]. A set of 100 ns simulation of Na^+ and POPC bilayer showed strong coordination of ions by the ester oxygen of the lipids by

another study[8]. A notable study for anionic lipid membrane 1-Palmitoyl-2-Oleoyl-sn-glycero-3-Phospho (1′-rac-glycerol) (POPG) interactions with Na^+ and K^+ plus Ca^{2+} has shown that the sub microsecond simulation time is needed to meaningfully capture the ion-lipid interactions with multiple conformations[9]. In fact, the binding here refers to two phenomena. First, the ion should be electrostatically attracted to the surface of the bilayer and then the adsorption binding happens between lipid headgroups and the ion. The kinetics of binding usually characterized by deuterium magnetic resonance is reported to be fast (less than 10 μs) and involves one Calcium coordinates with two lipids[10].

ITC experiments have been done on POPG/POPC under the liquid crystalline phase only in order to avoid the heat associated with a phase change[11]. In this research, authors reported that calcium binding to pure POPC is weak, and the binding constant is near $1M^{-1}$, however, adding 25 % of POPG to the vesicles yields a positive enthalpy of binding. The vesicle size and method of preparation had minimal effect on the final result. Again, this study did not provide an atomistic picture on how the binding occurs even if the enthalpy was not the main driving force for binding.

In this study, we further prove Isothermal Titration Calorimetry as a reliable experimental approach to characterization of the binding thermodynamics of divalent ions Ca^{2+} and Be^{2+} to phosphorylated compounds such as those in negatively charged lipids POPG, POPS (1-Palmitoyl-2-Oleoyl-sn-glycero-Phospho-L-serine) and POPA (1-Palmitoyl-2-Oleoyl-sn-glycero-3-Phosphate). In our experiments, these anionic lipids were studied as a mixture with neutral

lipid POPC (Fig. 1) for liposome stability (POPC is zwitterionic and abundant in cell membranes and helping to stabilize negatively charged lipids). But before approaching phospholipids, we explored in detail binding of these ions with two small molecules chosen to emulate two types of phosphates present on lipids head groups. This is Glycerol-3-Phosphate (Gly3P) with a terminal headgroup similar to that of POPA and Dimethyl Phosphate (DMP) with a similar phosphate configuration as in most common phospholipids, POPC, POPG and POPS. Hence, these two small molecules guide us to better interpret the binding of lipids negatively charged phosphates to ions at different pH values. Gly3P, as seen in Fig. 2, has two dissociable protons and three protonation states, whereas DMP has only one hydrogen capable of deprotonation. The important point here is to acknowledge the ability of beryllium to deprotonate hydroxyl hydrogen[12]. This ability could lead to accompanying processes producing additional heat generation during ITC experiments since Be^{2+}makes multiple hydroxide species with water and can displace H^{+} in many strong hydrogen bonds.

We find it important that the 'acceptor' phosphate groups have multiple protonation states and that free Be^{2+} ion is capable of hydrolyzing water and coordinating several hydroxyls. On binding to phosphoryl oxygens, Be^{2+} is expected to deprotonate some of them, which will lead to H^{+} release, but at the same time, Be^{2+} will shed OH^{-} groups which may recombine with protons. For this reason, *a-priori*, the outcome cannot be easily predicted and so we designed experiments with unbuffered, weakly buffered and more strongly buffered solutions. We do not treat the contributions of protonation-deprotonation reactions quantitatively but simply try find consistency between experiments performed at different pH. Deconvolution of different heat contributions will be a task for the future.

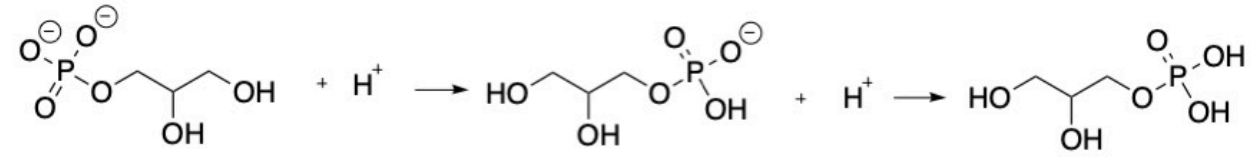

a) Glycerol 3-Phosphate

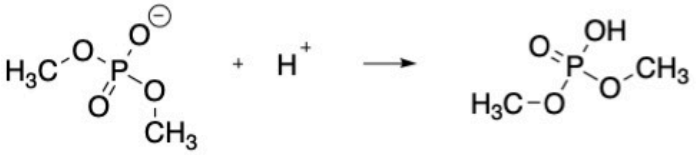

b) Dimethyl Phosphate

Figure 2. Glycerol Phosphate and Dimethyl Phosphate investigated in this study drawn by CHEMDRAW

Chapter 2: Materials and Methods

Isothermal Titration Calorimetry (ITC)

ITC is a powerful tool to measure the binding heat in a label-free fashion. In this work, we were able to measure the heat associated with binding of ions with small model compounds and liposomes. All measurements were done on a Microcal VP-ITC calorimeter (Malvern) at 25 $°C$, and the fitting of thermograms was done using the pre-installed Microcal Origin software. Solutions of $BeSO_4$ and $CaCl_2$ have been prepared in either 2 mM or 10 mM Tris buffer supplemented with 2 mM KCl as a low-ionic strength background electrolyte. In typical experiments, 20 μl injections were introduced in a 1.4 ml calorimetric chamber with 300 s time intervals.

Lipids were purchased from Avanti Polar Lipids, Birmingham, AL and kept in -20 $°C$ freezer before preparation process. Small unilamellar vesicles (SUVs) were prepared by rehydration and sonication of a lipid film formed on the wall of a 10-ml round-bottom glass tube. For this, lipids dissolved in chloroform were dried on the tube wall under a stream of nitrogen followed by at least a 6-hours drying under vacuum in a desiccator. Lipids were re-hydrated in the buffer and the suspension was vortexed and sonicated for 10 minutes with shaking in the ultrasonic bath. The liposomes were dialyzed overnight in 500 ml of the same buffer, which was then used to prepare stocks of phosphate compounds for ITC. The dialyzed liposomes were diluted to 2.5 mM and used for ITC titration afterward. For calculations, the outer surface of liposomes exposed to

ions was taken as 55% of the total concentration of lipids and corrected before the fitting procedure in Origin. The size of vesicles was 140 (± 10) μm as measured by dynamic light scattering (DLS) on a NanoBrook Omni (Brookhaven Instr).

Analysis of ITC data

Fitting of all thermograms was done using the Microcal Origin software. In this method, the interaction between macromolecule and ligand could be measured accurately in one experiment[13]. The most precise parameter obtained by this method is the heat released or absorbed during the reaction. A series of 14 or more 20-ul injections of ligand were injected from the syringe into the 1.4 ml chamber and the peaks of heat observed at each injection were integrated. The integrated heat then plotted against the ratio of ligand to macromolecule concentration which is increasing over the course of reaction (known as binding thermograms). The binding heat is directly obtained from the plot; however, the binding constant and the entropy changes are calculated indirectly from the shape of thermograms (will be proved shortly). Having the binding constant which is the slope of inflection point of isotherms curve, it is possible to calculate the entropy by the Gibbs formula $\Delta G = -RTlnK = \Delta H - T\Delta S$. This powerful technique allowed us to characterize the nature of binding for each system of interest and repeating each experiment three or four times enabled a trustworthy data collection.

Each isotherm integrated to produce one point on the graph which we fitted by either one binding site model (1:1 model of binding from now on) or two binding sites model (1:2 model) in calorimetric experiment. The derivation of formula will be provided here for 1:1 binding, and the two binding sites model derivation follows the same thermodynamics principles. In 1:1 binding: $M + L \leftrightarrow ML$ and we can write $M_T = [ML] + [M]$ in which [M] is free unbounded macromolecule. Also, we have the ligand formula $L_T = [ML] + [L]$ and again [L] is the free ligand concentration. Thermodynamic equilibrium constant implies that: $K = \frac{[ML]}{[M][L]}$. By substituting [L] and [M] into binding constant we then get a quadratic formula to solve for [ML]: [ML]=$\frac{-b \pm \sqrt{b^2 - 4ac'}}{2a}$ where $b = \frac{-1}{K} + [M_T] + [L_T]$, $c' = [M_T][L_T]$ and $a = 1$. By taking derivative of [ML] with respect to $[L_T]$ and considering that $dQ = d[ML].V_0.\Delta H^0$ (where ΔH^0 is binding enthalpy and V_0 is the chamber volume), we can get the y-axis which is:

$\frac{dQ}{d[L_T]}.\frac{1}{V_0} = \Delta H^0 \times [\frac{1}{2} + \frac{1 - \left(\frac{C+1}{2C}\right) - \frac{P}{2}}{\sqrt{P^2 - 2P\left(\frac{C+1}{C}\right) + (\frac{C+1}{C})^2}}]$, where $c = [M_T]K$ and $P = \frac{[L_T]}{[M_T]}$. If we take another derivative, then the slope of inflection point is: $-\frac{1}{4}\sqrt{c}.\Delta H$ and one can get c value and corresponding K_a value either by geometric analysis[14] or by fitting. P value is nothing but x-axis and by plotting against y-axis we can fit this model to data and extract required parameters.

This is the basic fit used in Wiseman isotherms and it has an instructional purpose; however, the Origin software uses more complex equation to take into account the dilution after each injection and the fitting needs more sophisticated procedure. Here, we refer to the manual of ITC MALVERN, FITTING PROCEDURE which is available online for free to download (https://jeltsch.org/sites/jeltsch.org/files/files/MicroCal-PEAQ-ITC-Analysis-Software-User-Manual-English-MAN576-01-EN-00.pdf). This needs a good guess for parameters such as n, K, ΔH or ΔS. Finding a good guess specifically is not a trivial task. The way fitting performed for two binding sites model was to first remove the binding points for second binding phenomenon and fit the data with one site model and then use these binding parameters as good guesses to fit the overall binding isotherm with all parameters from two binding phenomena simultaneously.

Chapter 3: Results

All ITC data are taken three times and only one curve has shown here. For more data please look at Appendices section. This chapter will start with a presentation of small molecules interactions with ions to illustrate different binding mechanisms. This will provide us a basis for experiments with liposomes allowing for meaningful comparison and data interpretation. Since the previous work from the Sukharev's lab[5'3] focused on carboxyl and phosphodiester groups binding to Be^{2+} represented by sodium acetate and dimethyl phosphate respectively, here we represent the data in the same manner for both beryllium and calcium ions with the focus on two types of phosphate groups. For this purpose, two small molecules have been chosen for ITC such that the differences between two phosphate groups at different pH values represent the distinct headgroups of lipids (which we will discuss in the following subsections).

Small Molecules

Glycerol 3- Phosphate (Gly3P):

The very first experiment was designed with solutions for which no special adjustment of pH was done. To estimate what may happen in the ITC chamber, we performed a 'mock' titration for which the pH changes with each injection could be directly measured with a miniature pH electrode. The concentrations of each of the components and the buffer composition were identical to those used in real ITC titrations. The data representing the course of pH change

during titrations are shown in table 1, beginning with pH 4.76 of buffered 1 mM $BeSO_4$ (line one) and ends with pH 6.48 after the last (14th) injection of Gly3P. The real ITC thermogram that was taken under identical buffered conditions is shown in Fig 4.

To understand the observed pH change, we performed a simple titration experiment, in which initial solution of Gly3P was titrated with HCl (Fig. 5). Consistently with the previous data for Phosphoric Acid[15], the terminal monoester phosphate group of Gly3P displays a two-wave titration curve with the first 'buffering' midpoint at pKa_1= 6.21 and the second wave with pKa_2 = 1.89. Therefore, mixing 1 mM of acidic $BeSO_4$ with 10 mM of Gly3P takes us close to the first titration midpoint (6.1-6.4), i.e., center of the first phosphate buffering zone. This range of pH values is within the first buffering region of Gly3P and the relative concentration of Gly3P compounds could be obtained by Henderson-Hasselbalch equation $\frac{[\mathrm{Gly3P^{2-}}]}{[\mathrm{Gly3P^{1-}}]} = pH - pKa_1$. ΔH is negative at the beginning for first binding site and this binding is enthalpically driven, however the second binding site has positive enthalpy and driven entropically which is more expected since Ca^{2+}shows the same behavior as can be seen in Fig. 7 ($CaCl_2$ has a pH value of 7.2 and titrated with Gly3P with pH value of 8.5 and the protonation state is similar to second binding site of $BeSO_4$ and Gly3P). At higher pH values Gly3P is already deprotonated, and the binding enthalpy does not contain a large contribution from protonation/deprotonation heat.

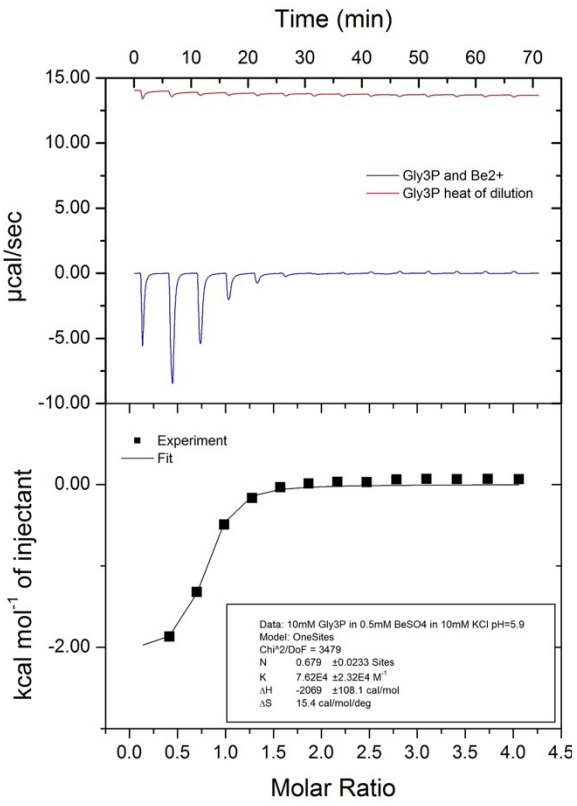

Figure 3. 0.5mM Gly3P and 10mM $BeSO_4$ in 10mM KCl and pH=5.9

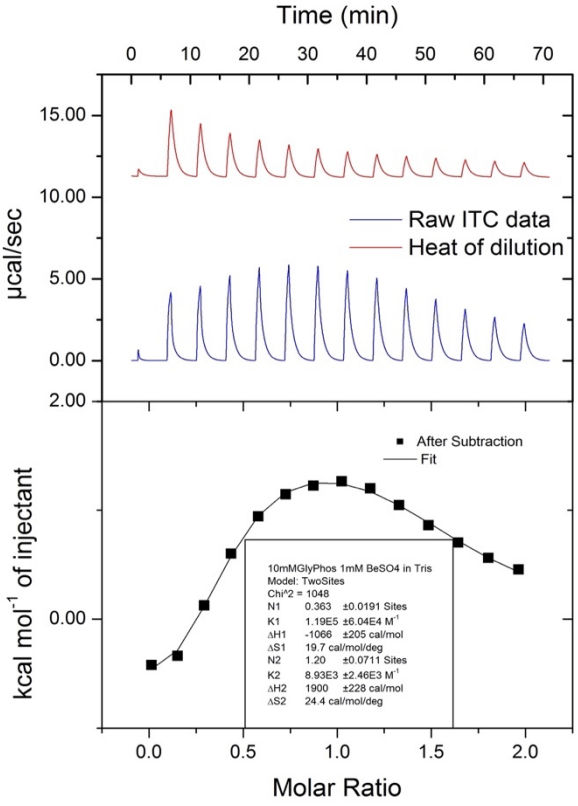

Figure 4. 10mM Gly3P and 1mM $BeSO_4$ in 2mM Tris 10mM KCl

Therefore, it is reasonable to consider that at pH above 6.2, both oxygens become deprotonated and it might be reasonable to assume at least two binding configurations stipulating a two-site fitting procedure of Gly3P-Be^{2+} thermograms.

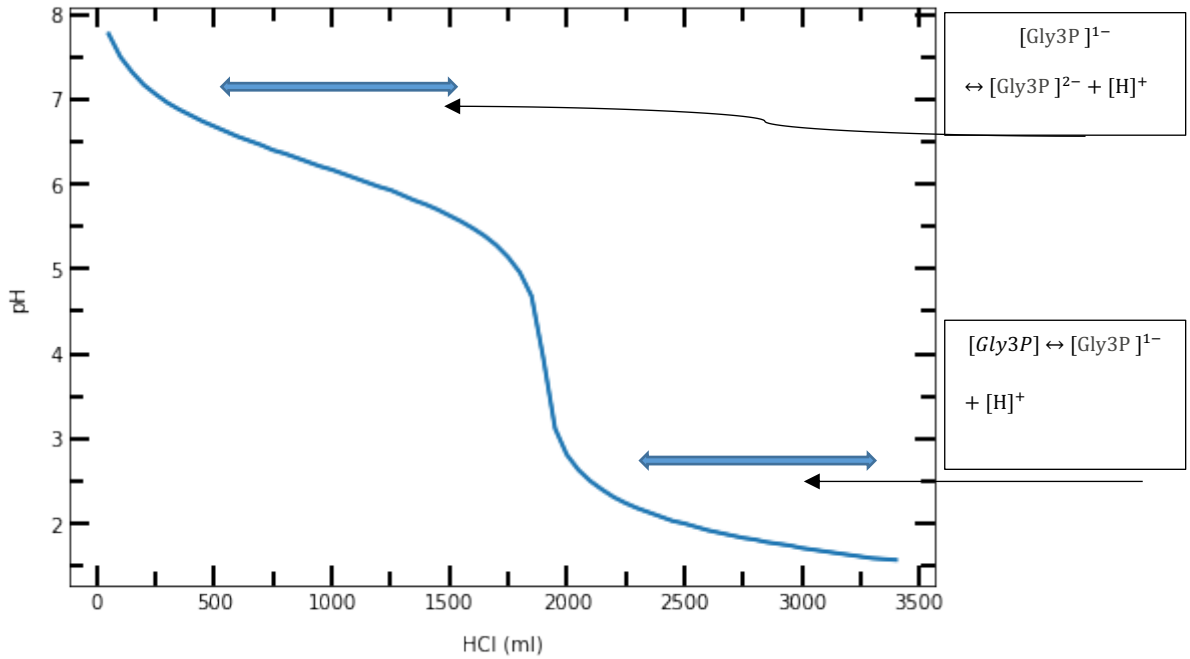

Figure 5. Titration curve for Gly3P with 1M HCl shows two binding sites with pKa1=6.21 and pKa2=1.89 values for protonation states of this molecule at different working pH values. The binding constants then acquired by ITC for further thermodynamics analysis (took only once)

At pH=5.9, Gly3P solution is mostly consists of $[\mathrm{Gly3P}\,]^{1-}$ according to our titration data and the heat contains the Be^{2+} interaction with H^{+}. The first scenario where pH left to change during the reaction, two populations are dominated with their own binding constants appeared in our isotherms. Interestingly, the second binding site is tighter than the first one, but we cannot draw any conclusion on heat released form deprotonation phenomenon as we discussed in first chapter.

Table 1. pH measurement of 10mM Gly3P and 1mM $BeSO_4$ shows possibility of protonation heat contribution to ITC enthalpy took only once.

Volume of titrant in microliter (Glycerol Phosphate)	pH	Spacing Time between injections in min
1	4.76	1
20	4.87	5
20	4.9	5
20	4.97	5
20	5.03	5
20	5.1	5
20	5.26	5
20	5.51	5
20	5.82	5
20	5.97	5
20	6.14	5
20	6.28	5
20	6.37	5
20	6.48	5
Final	6.48	5

To probe the possibility of aggregation and the expected positive enthalpy interaction, we have designed experiments with 5-to-10-fold diluted Gly3P and ion solutions. The result for the 10-fold diluted Gly3P is shown in Fig 6. The plot has been fitted with two binding sites both of which with positive enthalpy and entropy which indicate liberation of water as a major binding consequence. It seems that the binding isotherms corresponding to Ca^{2+} and Gly3P is very similar to this plot in nature. More elaboration needed in case of Gly3P and Be^{2+} and more points needed to reach the best fit in this case. Ca^{2+} affinity to Gly3P is 10 times lower than second binding site of Gly3P and Be^{2+} and 100 times lower than the first binding site of Gly3P and Be^{2+}.

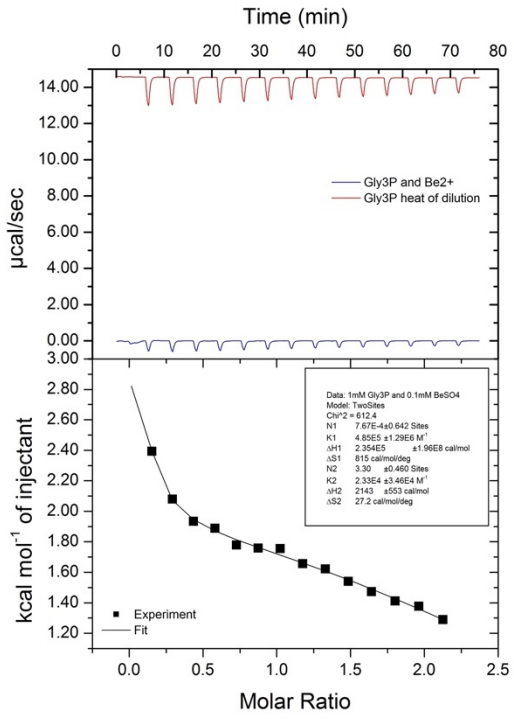

Figure 6. 0.1mM $BeSO_4$ and 1mM Gly3P in 2mM Tris 10mM KCl pH not accurate but around 6

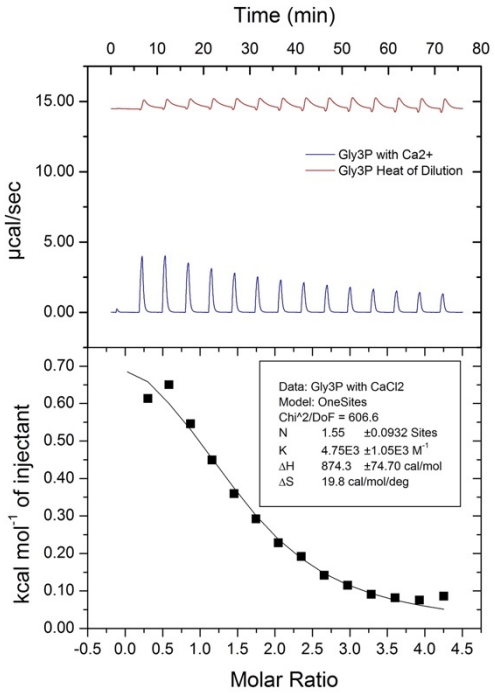

Figure 7. 0.5mM $CaCl_2$ titration with 10mM Gly3P in 2mM Tris 10mM KCl buffer pH=7.3

The second series of experiments has been designed so that the pH values for both titrant and titrate were carefully adjusted to be the same to minimize the effect of proton exchange. 0.5 mM of $BeSO_4$ - 10 mM KCl solutions were prepared and adjusted to pH=5.9 by adding a tiny amount of KOH. A 10 mM Gly3P solution in the same buffer was prepared and adjusted to pH=5.9 by adding HCl. At the end of the ITC, the chamber's content pH was 5.75 which shows no significant proton release or uptake during ITC injections (Fig 4). To get a more vivid picture on the effect of pH on Gly3P and Be^{2+} binding, we chose to measure the pH during the course of

the reaction for 1mM Gly3P and 0.1mM $BeSO_4$ and found no significant pH change fluctuate around 6. The most reliable data comes from Fig.4 and we spend the rest of this section to try interpret them.

At pH=5.9, based on Henderson-Hasselbalch equation the ratio of charged Gly3P is $\frac{[\mathrm{Gly3P}^{2-}]}{[\mathrm{Gly3P}^{1-}]} = 0.49 \approx 0.5$ and the effective charge of Gly3P is -1.33 at this pH value. This titration (Fig 4) best fitted with one site model and negative ΔH shows that the electrostatic interaction of Be^{2+} and Gly3P phosphoryl oxygens overpowers the liberation of water from both groups (breaking bonds between solvated solutes and water which require energy) and drives binding phenomena.

The next step could be to have data at pH=3 which may illustrate the ability of Be^{2+} to deprotonate partially protonated oxygens of Gly3P. This heat of reaction and the pH at the end of the ITC may estimate the number of liberated protons in our system.

.

Dimethyl Phosphate (DMP):

Multiple ITC experiments have been designed to get a reliable binding energy between DMP and Be^{2+}. First, we have tried 4mM DMP and 2mM $BeSO_4$, however, at the end of the titration there is another binding probably due to aggregation (Fig. 9). Diluted solution of 1mM $BeSO_4$ and 0.5mM DMP on the other hand, has a smooth curve very well fitted

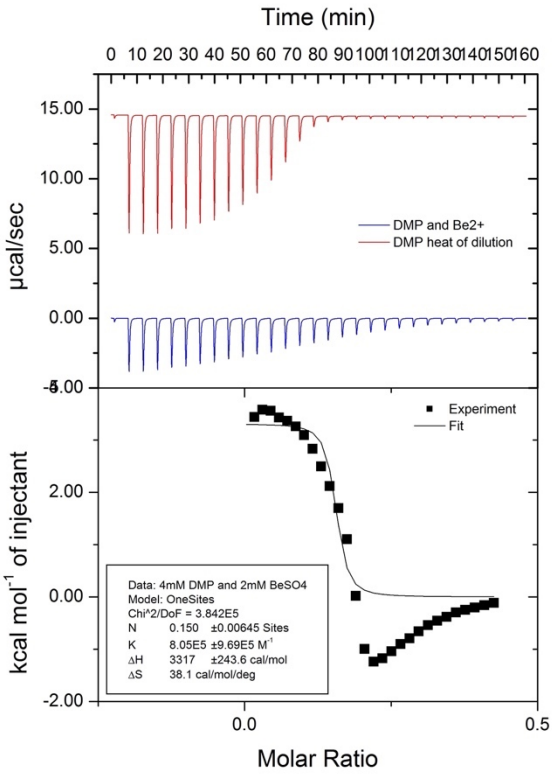

Figure 9. 4mM DMP and 2mM $BeSO_4$ in 2mM Tris 10mM KCl

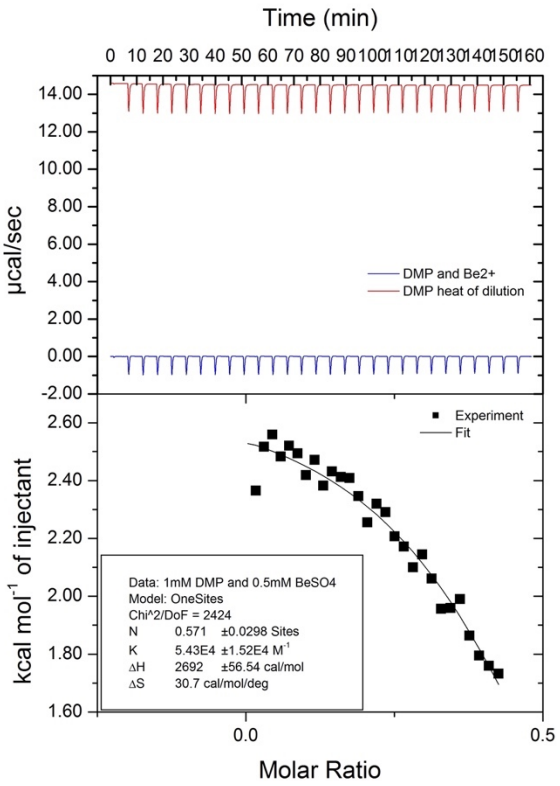

Figure 8. 1mM DMP and 0.5 mM $BeSO_4$ in 2mM Tris 10mM KCl

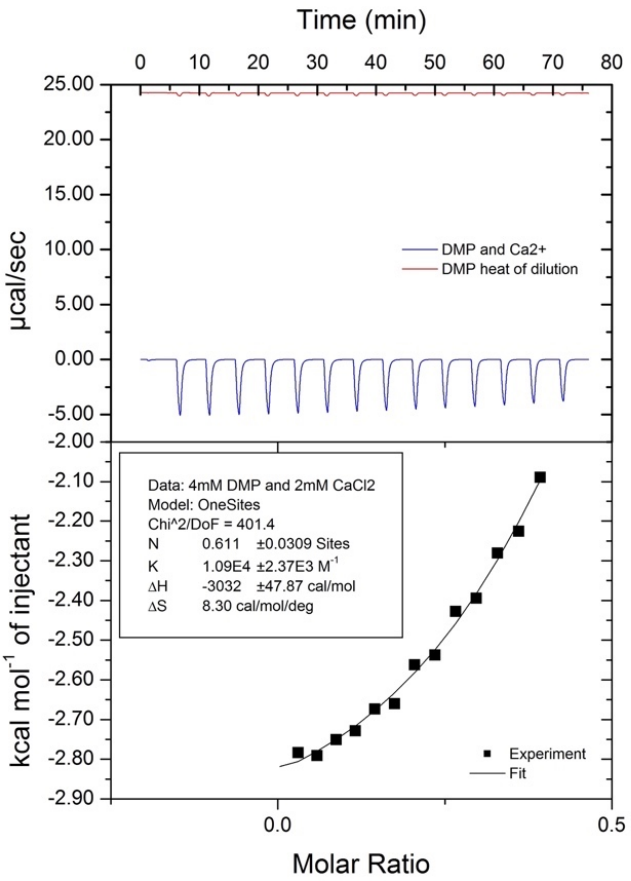

Figure 10. 4mM DMP and 2mM $CaCl_2$ in 2mM Tris 10mM KCl

with one binding site (Fig. 8). Higher heat of dilution of DMP in buffer reversed the heat of binding to a positive heat and the binding is entropically driven. Tighter binding of water to beryllium ion in the first and second solvation shell could be a possible explanation for this positive enthalpy in comparison with calcium ion. Fig 10. shows the binding isotherms of Ca^{2+} and DMP.

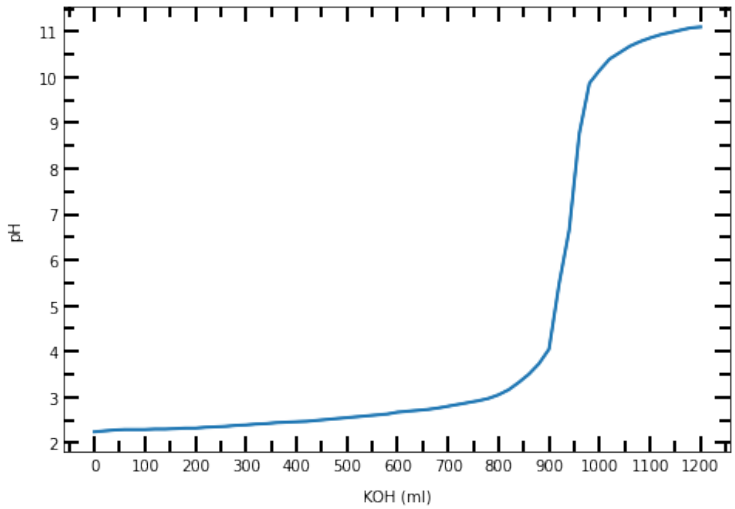

Figure 11. DMP titration curve. Arrows show the buffer region used to calculate pKa value at half equivalence point of each molecule. 10mM DMP solution has been used for this experiment (took only once)

The negative enthalpy implies that upon binding of ions to deprotonated oxygen of DMP, the energy of electrostatic interactions is much higher than the energy required to disrupt the water shell around ion and molecule. The less positive entropy remains as an open question since Ca^{2+} has a higher coordination number than Be^{2+}. Furthermore, it does not show the same behavior in compare with Gly3P (at which binding occurs by more liberation of water and a positive enthalpy Fig 7.) even if we expect higher electrostatic interactions and lower enthalpy between Gly3P and Ca^{2+} at neutral pH.

Another explanation could be related to the fully deprotonated phosphoryl oxygens in Gly3P at high pH which implies tighter water molecules around it. The tighter the bonds the more energy is needed to release them upon ion binding. In the case of DMP, however, less energy needs to compensate for water bonds breaking around oxygen.

Summary of ITC experiments are provided below with standard deviation of 3 independent trials for each data:

Table 2. ITC results summary for ion-small molecule experiments with ± one standard deviation

Experiments repeated three times	K_a M^{-1}	ΔS (CAL/MOL/°)	ΔH (KCAL/MOL)
Be^{2+} + DMP	4.76E4 ± 0.67E4	30.4 ± 0	2.685 ± 0.08415
Be^{2+} + Gly3P Diluted version	K_{d1}= 1.57E7 ± 2.19E7 K_{d2}= 5.056E4 ± ± 4.06E4	ΔS_1= 361.36 ± 403.82 ΔS_2= 27.36 ± 0.86	ΔH_1= 2.9E2 ± 9.9E1 ΔH_2= 1.929 ± 0.211
Ca^{2+} + DMP	2.43E5 ± 2.93E5	-19.16 ± 23.7	-1.2487E1 ± 8.186
Ca^{2+} + Gly3p	3.133E3 ± 1.4 E3	21.5 ± 1.55	1.684 ± 0.0717

Liposomes

POPA/POPC (3:1)

POPA lipids are gaining more and more attention in recent years due to their ability to induce negative curvature in cell membrane first, and second the importance of Ca^{2+}-POPA interaction in cell fusion. PA-binding proteins and PA specific interactions through calcium binding with these proteins have also been characterized[16].

ITC performed on POPA/POPC (molar ratio 3:1) liposomes and binding isotherms with one binding site model shows 10 times higher affinity for Be^{2+} in comparison to Ca^{2+} at least in one of the buffers (Fig. 12 & 13). Each figure contains two titrations at low and high Tris concentration. Buffer with low buffer concentration is 2mM Tris and 10mM KCl and buffer with a higher buffer concentration is 10mM Tris and 10mM KCl. Interestingly, no effect of buffering strength has been observed in the case of POPA binding constants with both ions. The peaks are narrow which implies no secondary effects such as aggregation or fusion of liposomes. The last peak amplitude is zero indicating that the binding sites are fully saturated with ions at the end of the titration and the binding constant K_d=1-3 μM for beryllium ion was obtained by fitting a simple Langmuir adsorption one site model to experimental data. The lipid dilution heat is negligible, which is why the liposomes were titrated from syringe to the solution of salts in the chamber. Fig.13 shows that the calcium binding saturated at the end of the reaction and the stoichiometry of binding can be close to 'one to one'. However, Seelig et al.[10] measured the

quadrupole splitting of POPC choline head group upon addition of 5M Ca^{2+} and claims that the binding at saturation is one Ca^{2+} to two POPC lipids. Further investigation is needs for the case of POPA/POPC hence most of the interaction in our system comes from interaction of highly negatively charged POPA with ions rather than neutral POPC. The superficial interpretation is that the binding 1:1 corresponds to PA lipids with no contribution from PC since 75% of liposomes contain PA besides the higher electrostatic interaction of ions with PA.

Also, that study reported the effect of Na^{+} in binding of calcium as the buffer in the system. To avoid this complexity, we used a much larger ion K^{+} which interacts less with lipids in comparison with Na^{+}. Atomistic details of these interactions and the stoichiometry of binding will be needed by MD simulations. Obviously, Ca^{2+} binds to lipids with one order of magnitude lower affinity than Be^{2+} which is consistent with reported data for DOPS lipids[3].

Here we elaborate more on POPA data by comparing our results with Gly3P which has been chosen to represent PA headgroup. From our titration curves, Be^{2+} binds to Gly3P at pH value around 6 with $14\mu M$ affinity (Fig. 3) and the result for liposomes shows 30 times lower affinity with $K_d = 5\ \mu M$ approximately. This inconsistency comes from the fact that the data for small molecule should be treated more carefully regarding aggregation possibility and contribution heat from deprotonation.

Since the heat of reaction is also higher for Be^{2+} it is reasonable to consider higher electrostatic interactions of Be^{2+} with PA as the main driving force of binding phenomena.

The binding in both cases shows high affinity of ions to lipids due to divalent nature of cations, but in case of Ca^{2+}, binding is more entropically driven in contrast to Be^{2+} which seems to be more enthalpically driven. This is understandable if we bear in mind that the coordination number of Be^{2+} is 4 in comparison with Ca^{2+} with 6 water molecules in its first hydration shell. Releasing of water increases the entropy, however, more energy is needed which led to higher entropy and lower enthalpy for Ca^{2+} binding compare with Be^{2+}.

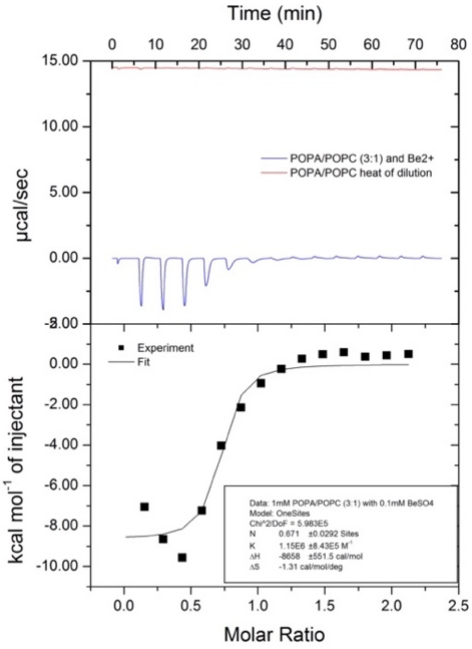

Figure 12. 0.1mM $BeSO_4$ and 1mM POPA/POPC (3:1) isothermal titration calorimetry in 2 mM Tris and 10 mM KCl buffer

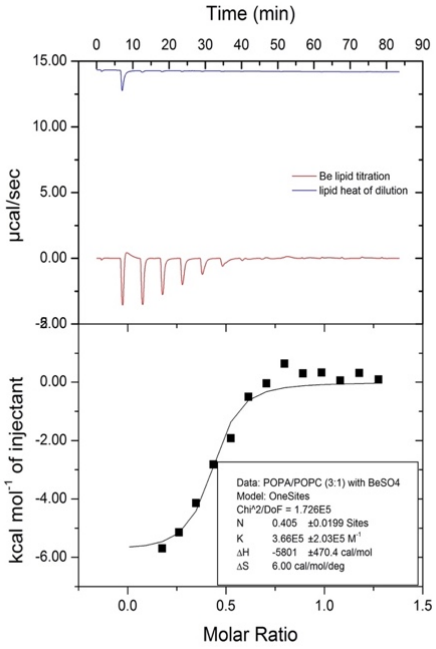

Figure 13. 0.1mM $BeSO_4$ and 1mM POPA/POPC (3:1) isothermal titration calorimetry in 10 mM Tris and 10 mM KCl buffer

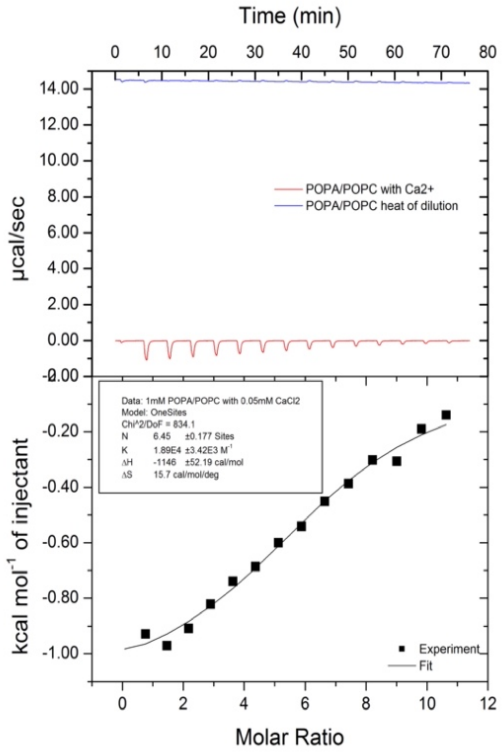

Figure 14. 0.05mM $CaCl_2$ and 1mM POPA/POPC (3:1) isothermal titration calorimetry in 2mM Tris and 10mM KCl buffer

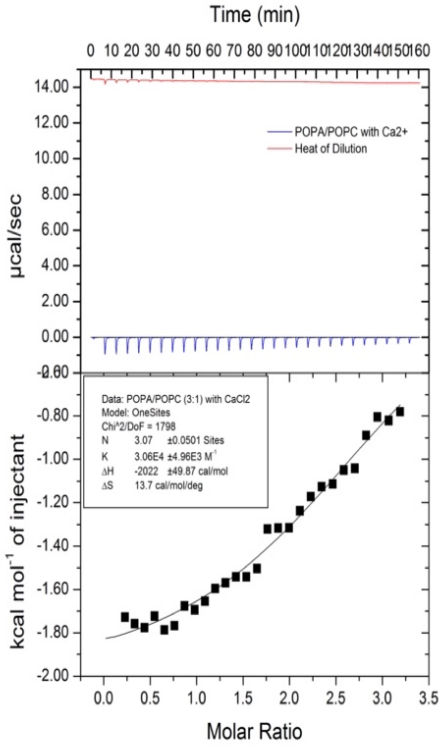

Figure 15. 0.05mM $CaCl_2$ and 1mM POPA/POPC (3:1) isothermal titration calorimetry in 10mM Tris and 10mM KCl buffer

Comparing this data with Ca^{2+}-Gly3P shows even more inconsistency in comparison with Be^{2+} data. The heat completely reversed in liposomes titration and the binding affinity is more realistic than small molecules (since small molecules binds with 4750 μM affinity and positive enthalpy which means there is a high contribution of desolvation phenomena in comparison with liposomes).

POPG/POPC (3:1)

Binding affinity for POPG/POPC (3:1) liposomes and Ca^{2+} could not be obtained in 10mM Tris 10mM KCl buffer. The titration in 2mM Tris and 10mM KCl revealed negative enthalpy and 10 times lower binding constant than POPA (Fig. 16). A binding affinity 10 times lower than POPA/POPC liposomes have been obtained from ITC experiments with Be^{2+} (Fig. 17).

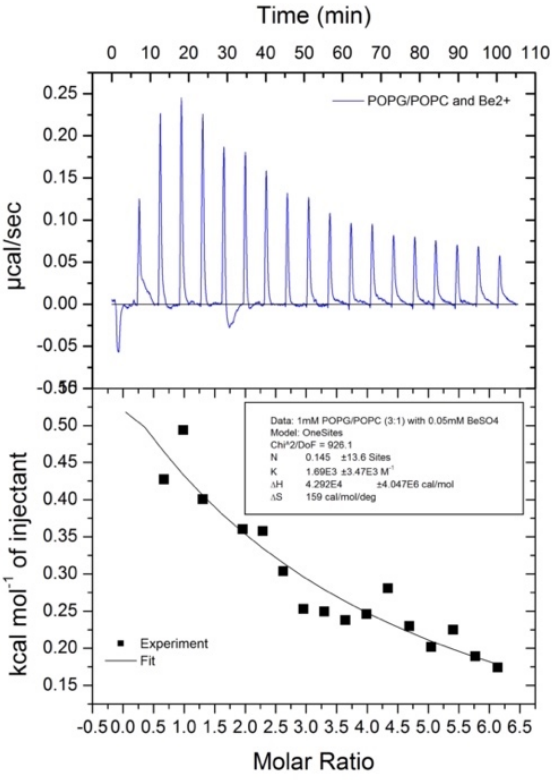

Figure 17. 1mM POPG/POPC (3:1) titration with 0.05mM $BeSO_4$ in 10mM Tris 10mM KCl

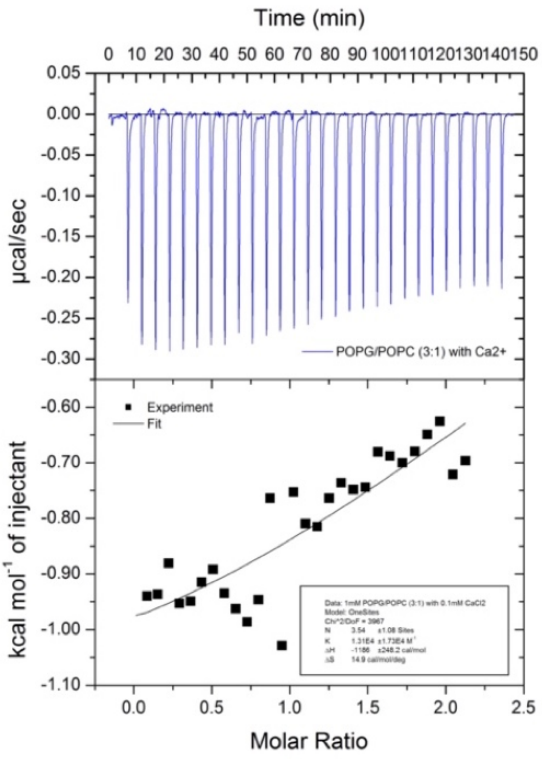

Figure 16. 1.5mM POPG/POPC (3:1) with 0.1mM $CaCl_2$ in 2mM Tris 10mM KCl

We conclude here that the 10 times higher binding affinity comes from higher electrostatic interaction of ions with two phosphoryl oxygens of lipids in POPA in comparison with POPG for both ions. In all experiments the binding phenomena were driven entropically associated with the release of water molecules from ions and lipid head groups. Positive enthalpy of Be^{2+} and POPG/POPC could be explained if we again consider that the liberation of water upon binding by Be^{2+} needs more energy than Ca^{2+}. The question that still remains to be address is whether the Be^{2+}can displace Ca^{2+} in displacement ITC of POPA/POPC and POPG/POPC.

In comparison with DMP data we can state here that the binding constants for Ca^{2+} is in good agreement between DMP and POPG. The same agreement exists for Be^{2+} data in which the heat released is comparable even if the binding constant is lower in lipids case.

POPS/POPC (3:1) and pure POPS

The next dataset would be the investigation of POPS lipids interaction with ions in ITC and probe the ability of Be^{2+} to interfere with Ca^{2+}mediated signaling processes in PS recognizing protein domains (Specifically Annexin V and Prothrombin proteins). POPS/POPC with 3:1 ratio has been used in ITC with Be^{2+} and Ca^{2+} ,however, Ca^{2+} does not show any binding.

Therefore, pure POPS and Ca^{2+} has been probed to get binding affinity. Even pure POPS should be prepared at low concentration to get reasonable binding constants. POPS and Ca^{2+} ion data was best fitted with two binding sites model, and it is possible that Ca^{2+} induced conformation change in lipid headgroup furnished different binding moieties for ion since it has

both acetate and phosphate oxygens. Entropy is positive for both binding sites implying dehydration effect or probably liquid crystalline phase shift has happened at the end of the ITC experiment. Fig. 18 shows the results for Be^{2+} and POPS/POPC. Again, the enthalpy is positive, and binding occurs with water liberation and the affinity is 10 times higher than of POPA/POPC

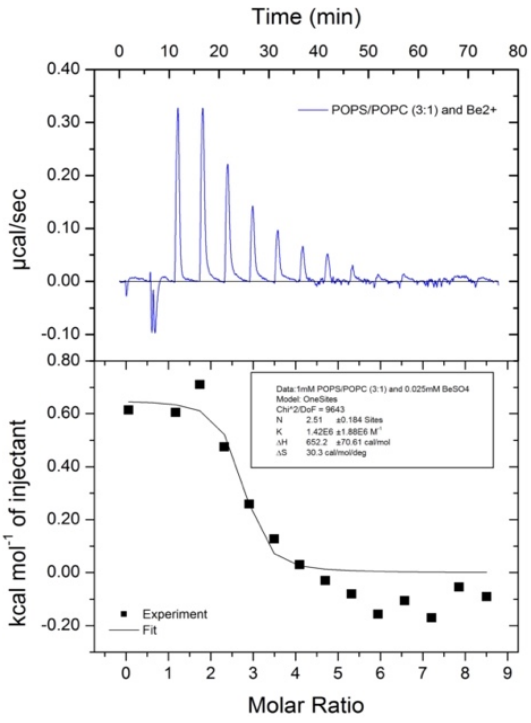

Figure 18. 0.025mM $BeSO_4$ and 1mM POPS/POPC (3:1) in 2mM Tris and 10mM KCl

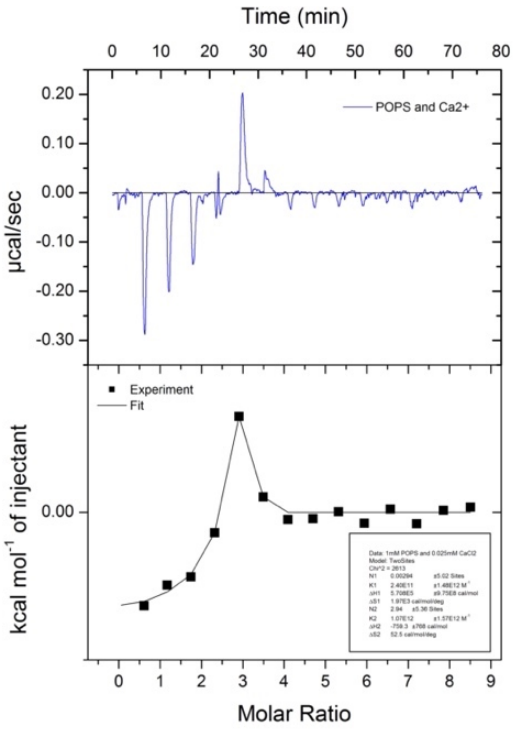

Figure 19. 1mM POPS and 0.025mM $CaCl_2$ in 2mM Tris 10mM KCl

(3:1) and about a 100 times higher than POPG/POPC (3:1). Only PA has negative binding enthalpy with Be^{2+} unlike PG and PS with Be^{2+}.

Summary of Liposomes ITC

Each experiment has been repeated 3 times except for POPG/POPC and calcium (2 times):

Table 3. Summary of results for ion-lipid experiments with ± one standard deviation

Experiments repeated 3 times	K_a M^{-1}	ΔS CAL/MOL/°	ΔH KCAL/MOL
Be^{2+} + POPA/POPC (3:1) in 10 mM KCl 10 mM Tris	1.67E5 ± 1.47E5	-0.85 ± 9.58 cal/mol/°	-7.285 ± 2.532 kcal/mol
Be^{2+} + POPG/POPC (3:1) in 10 mM KCl 2 mM Tris	1.05E4 ± 8.546E3	25.86 ± 6.27 cal/mol/°	2.216 ± 2.162 kcal/mol
Ca^{2+} + POPA/POPC (3:1) in 10 mM KCl 10 mM Tris	2.9E4 ± 1.32E4	13.19 ± 2.93 cal/mol/°	-2.075 ± 0.552 kcal/mol
Ca^{2+} + POPG/POPC (3:1) Only two replicates in 10mM KCl 2mM Tris	5.2E4 ± 5.5E4	19.56 ± 5 cal/mol/°	-0.676 ± 0.720 kcal/mol
Be^{2+} + POPS/POPC (3:1) 10 mM KCl 2 mM Tris	2.15E6 ± 1.8E6	29.5 ± 1.88 cal/mol/°	0.425 ± 0.163 kcal/mol
Ca^{2+} + pure POPS 10 mM KCl 2 mM Tris	Data will be provided in Appendices		

Chapter 4: Conclusion and future work

To summarize, we may state that the ITC phenomenology of ion binding to phospholipid liposomes and even to small model compounds mimicking the chemistry of the headgroups appears to be very complex. The reason is that ion-binding events to charged groups are always accompanied with substantial desolvation and transfer of protons. These may not distort the apparent K_d by orders of magnitude, but these 'hidden' reactions may change the manifestation of the primary binding event and obscure the driving forces. Yet, the comparison of experiments with model small compounds to experiments with liposomes emphasizes this difference between the apparent binding (dissociation) constant likely observed in liposomes that includes the effect of charged boundary and the presence of the electric double layer, and intrinsic binding constant likely observed in completely soluble model compounds. Understanding the presence of phase boundary and ordered orientation of headgroups would be the critical result of this comparison. There are many experiments that remain to be done for ion-liposome interactions by which the characterization of binding phenomena may become more complete and more realistic with the help of other experimental methods. The most relevant one is the electrophoretic experiment to get results for intrinsic binding constants. This could be done in accordance with a microsecond simulation with different force fields. Different binding moieties are present on the surface of the liposomes and characterization of binding phenomena to each moiety could be done by ITC at

different buffers to reduce the effect of buffer on the final results. More importantly, the binding of ion and competition mechanism between beryllium and calcium is of high interests.

Besides, the binding of proteins important for signaling mechanism could be then explored by refined force fields resulted from ITC work. This refinement is possible as we shown here for possibility of new phosphate group in our work comparing DMP and Gly3P.

Appendices

This section provides more ITC data used to calculate the standard error presented in table 2 for pure POPS and Ca^{2+} and a handful results shows the effective diameter of liposomes:

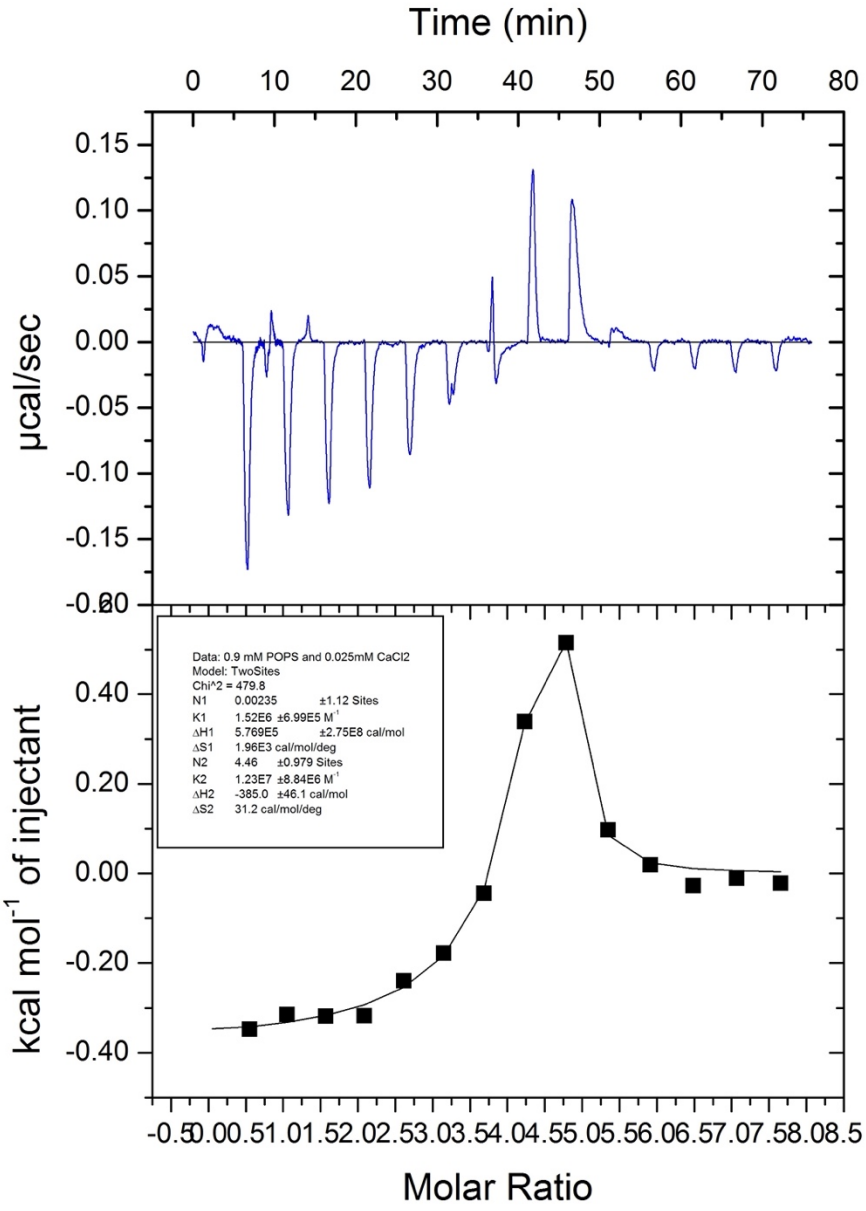

Figure S 1. POPS and calcium in 2mM Tris 10mM KCl

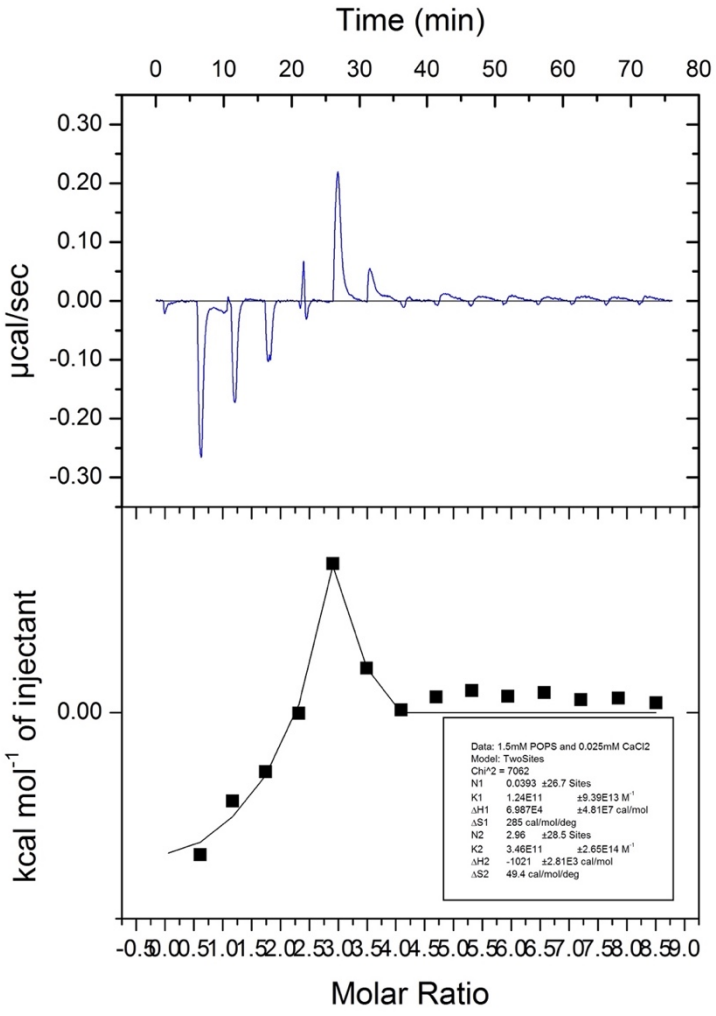

Figure S 2. POPS and calcium in 2mM Tris 10mM KCl

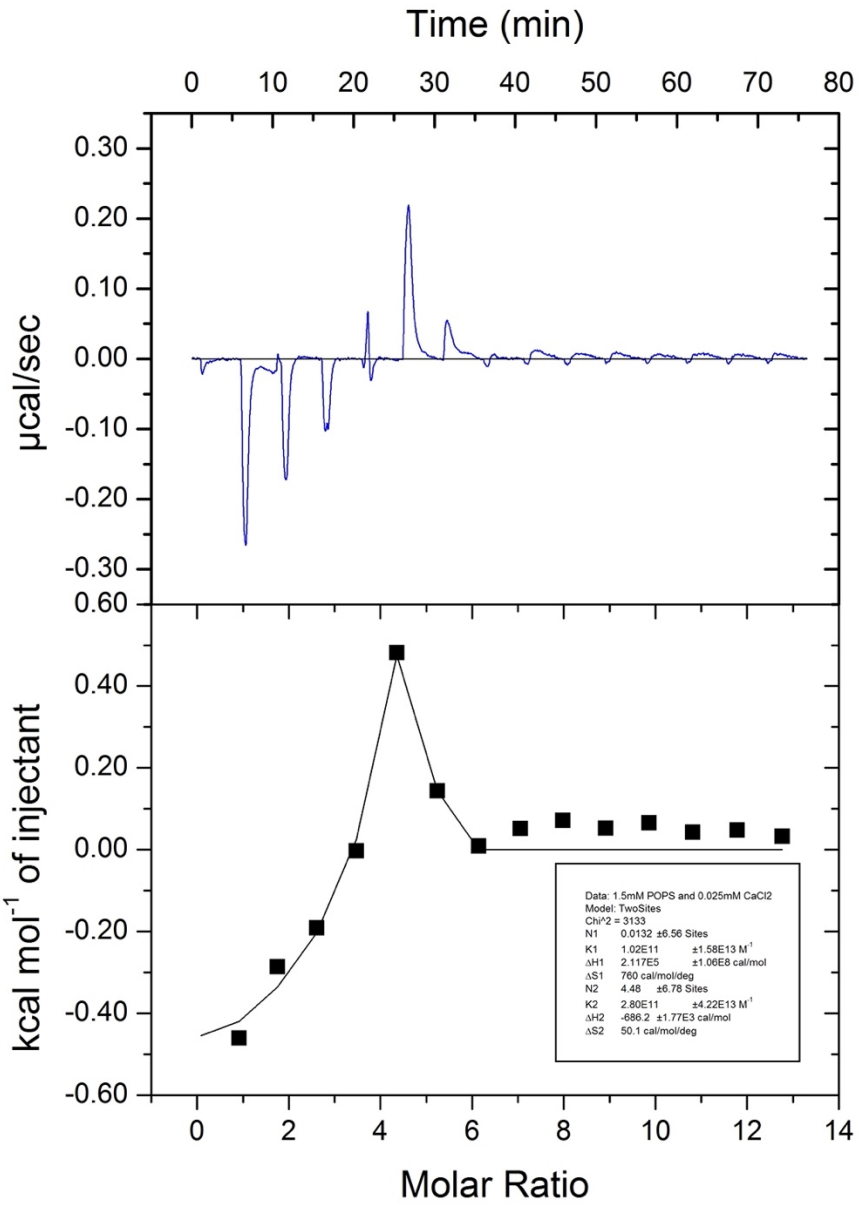

Figure S 3. POPS and calcium in 2mM Tris 10mM KCl

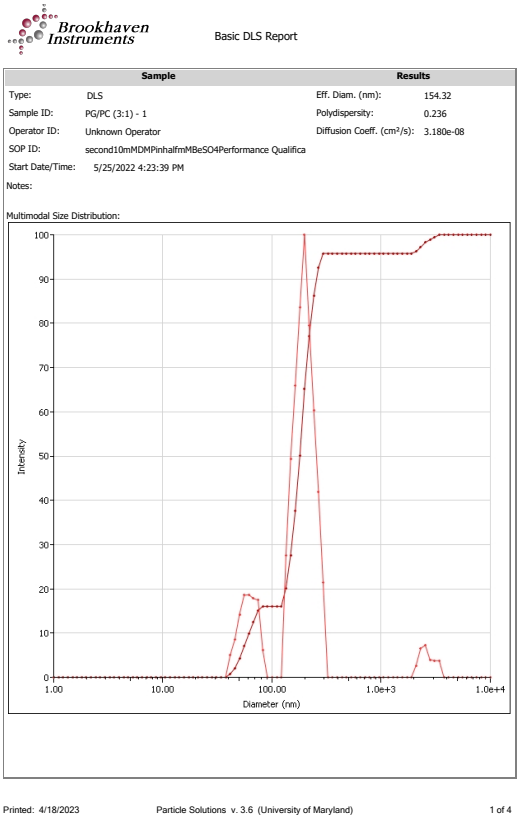

Figure S 5. POPG/POPC (3:1) effective diameter 154nm used in ITC from DLS

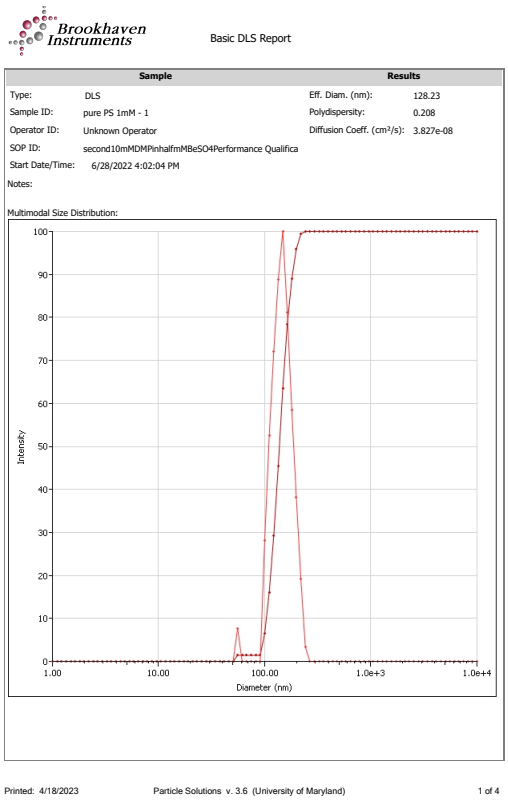

Figure S 4. Pure POPS liposomes effective diameter 128nm from DLS

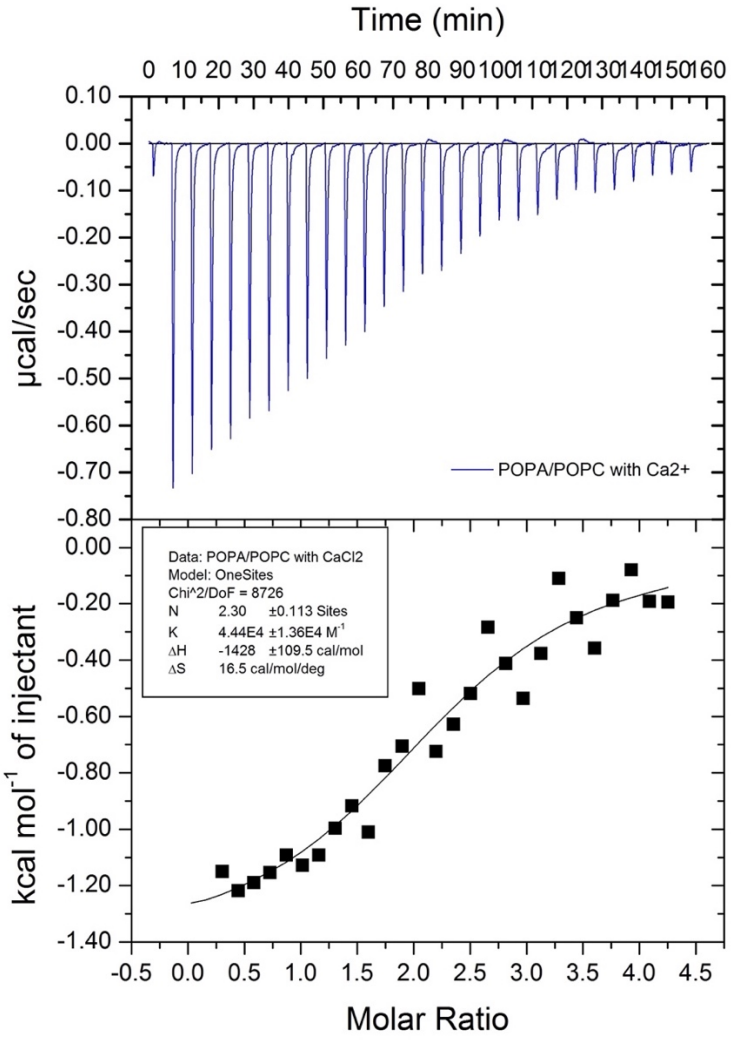

Figure S 6. POPA/POPC (3:1) and calcium in 10mM Tris 10mM KCl

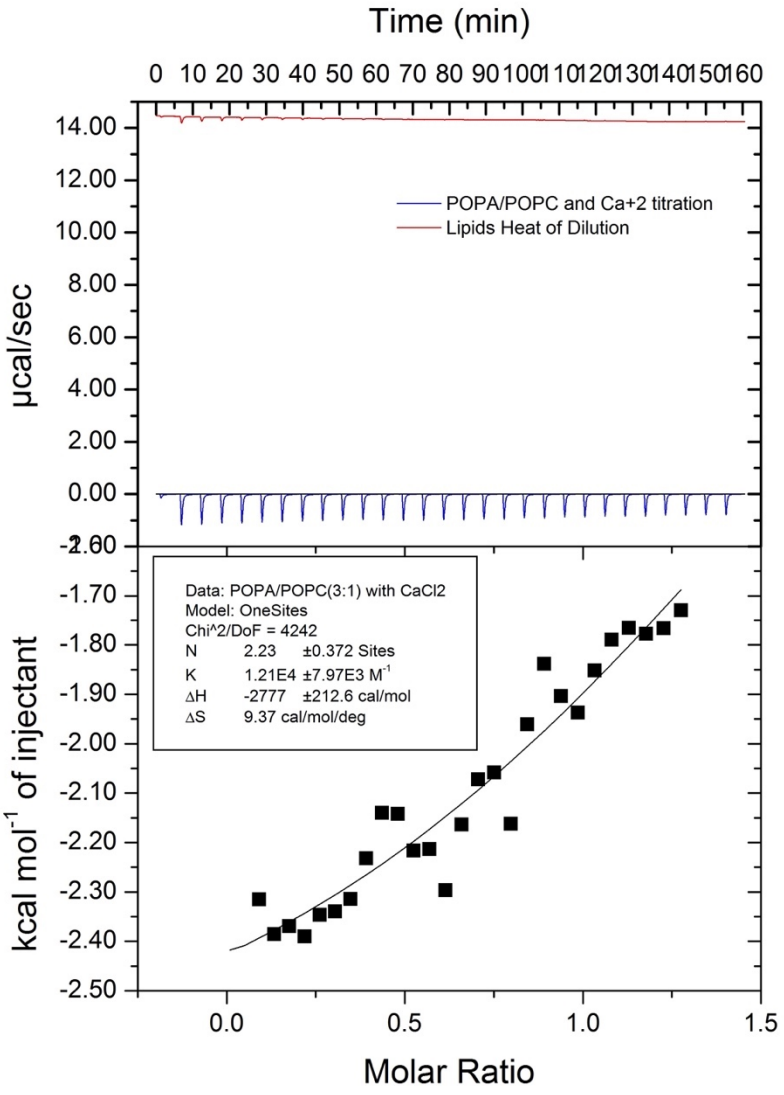

Figure S 7. POPA/POPC (3:1) and calcium with 10mM KCl and 10mM Tris

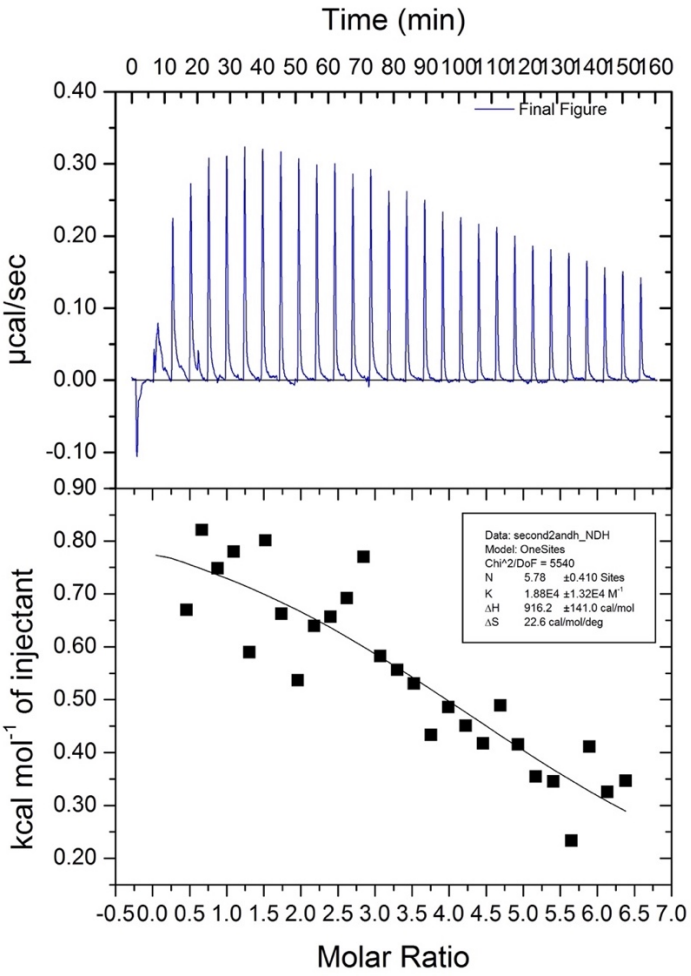

Figure S 8. PG/PC (3:1) with beryllium in 2mM Tris 10mM KCl

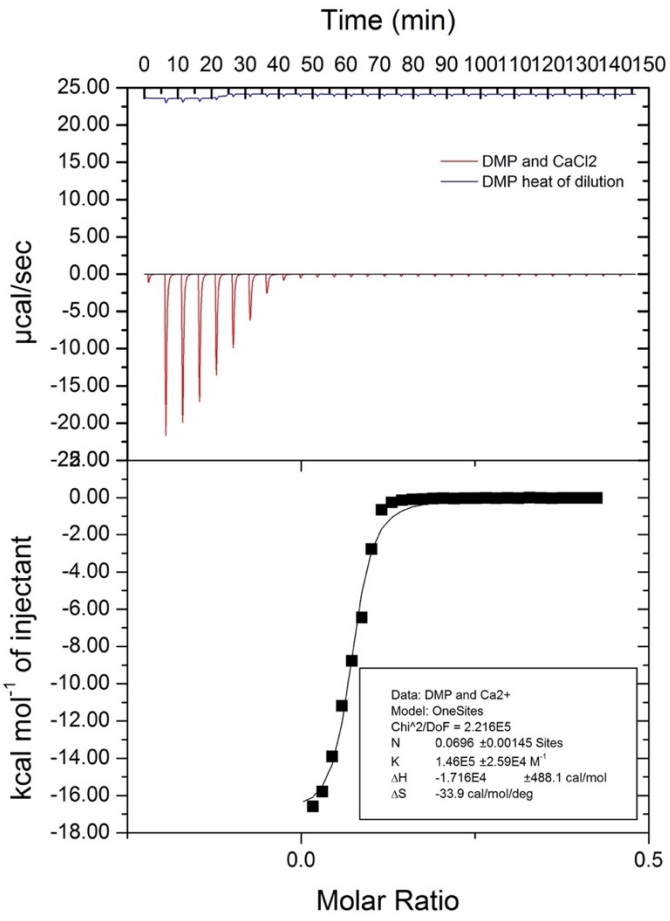

Figure S 9. 4mM DMP and 2mM CaCl2 in 2mM Tris 10mM KCl

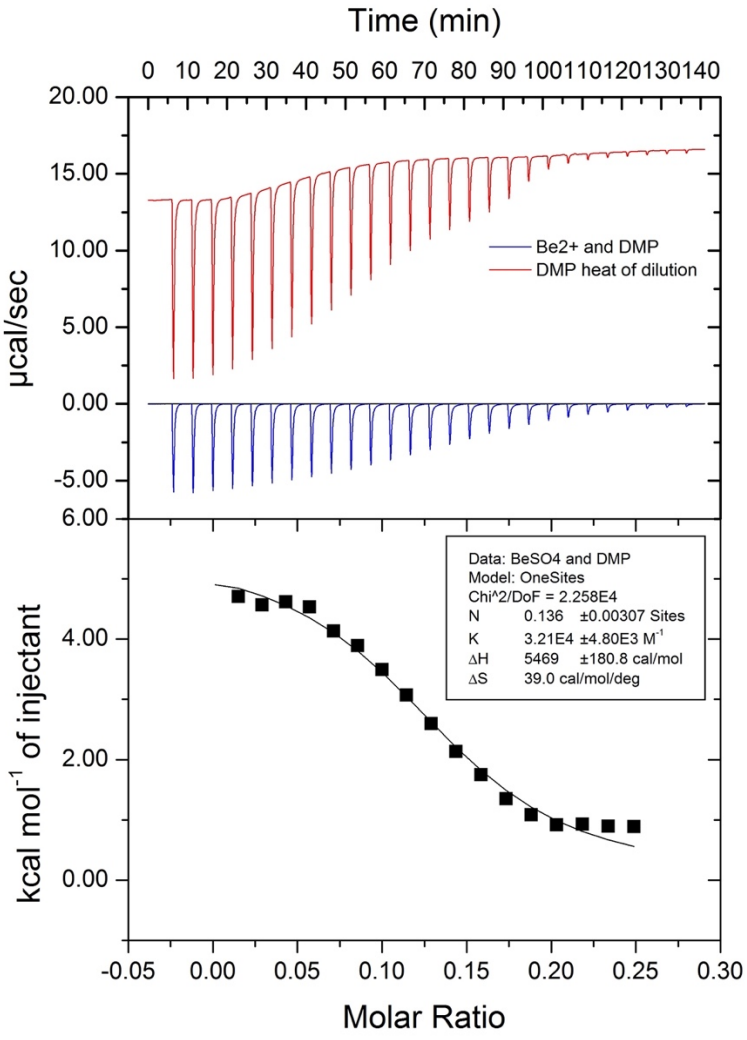

Figure S 10. 4mM DMP and 2mM BeSO4 in 2mM Tris 10mM KCl

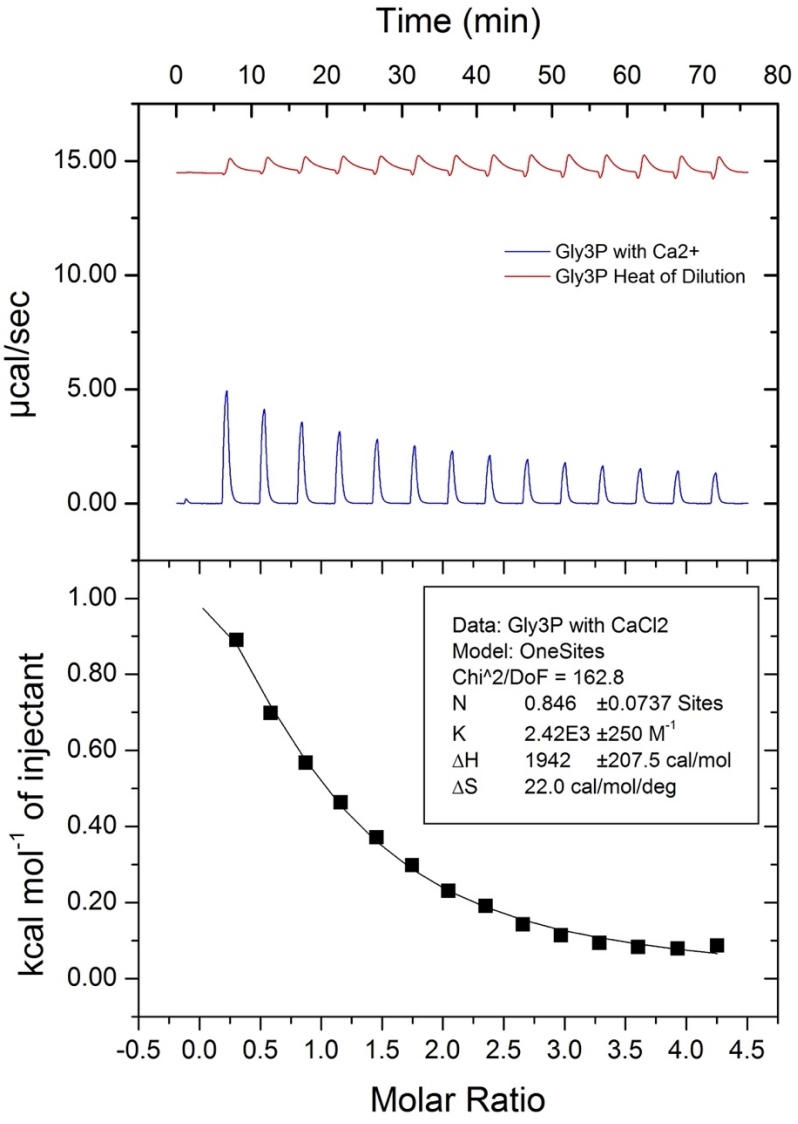

Figure S 11. 10mM Gly3P and 0.5mM CaCl2 in 2mM Tris 10mM KCl

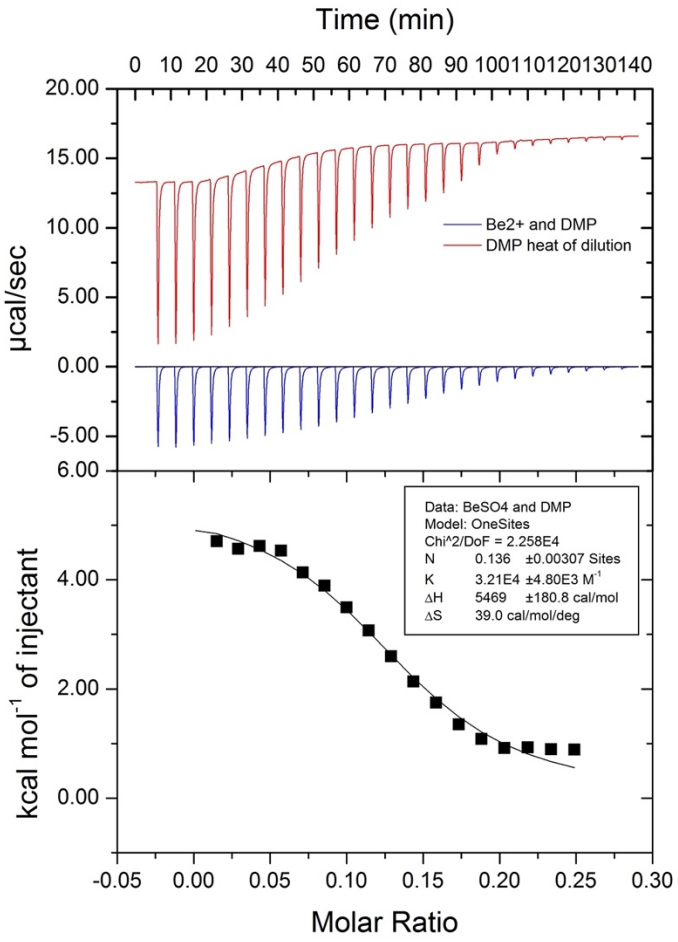

Figure S 12. 4mM DMP and 2mM BeSO4 in 2mM Tris 10mM KCl

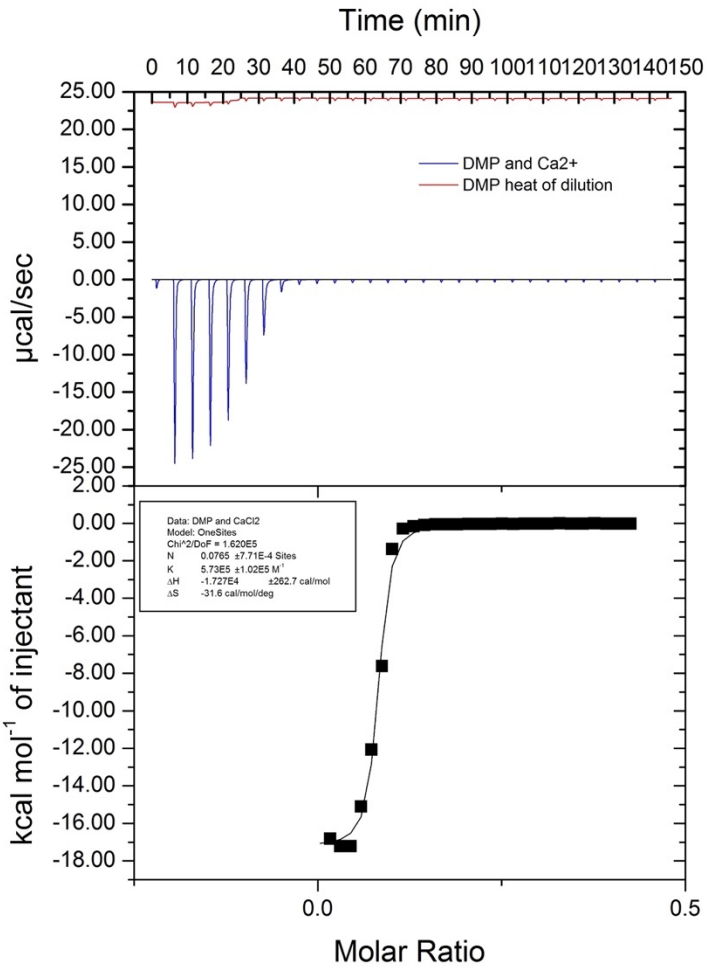

Figure S 13. 4mM DMP and 2mM CaCl2 in 2mM Tris 10mM KCl

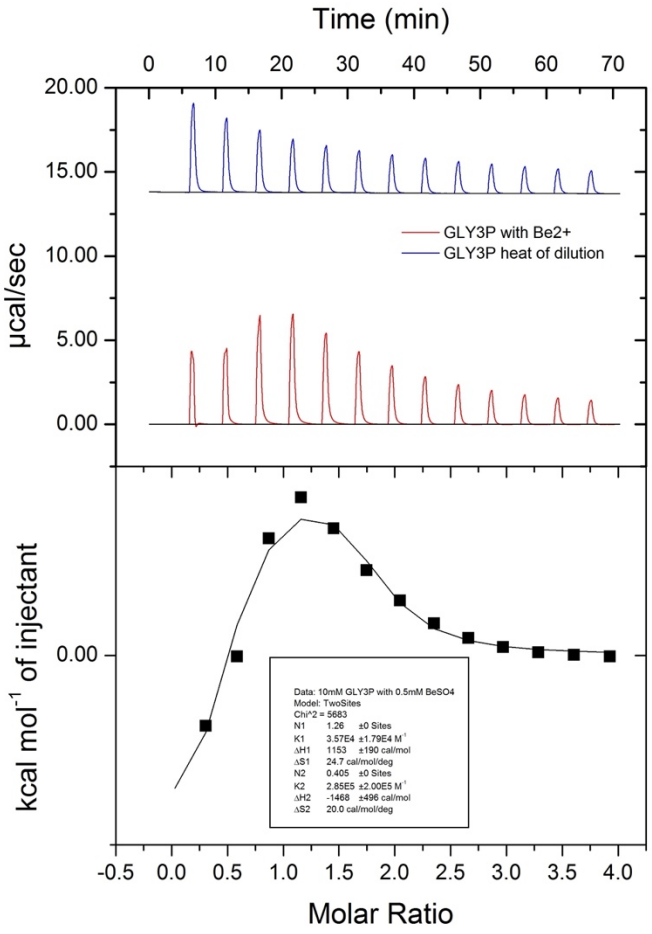

Figure S 14. 10mM Gly3P and 0.5mM BeSO4 in 2mM Tris 10mM KCl

Figures with caption Fig SS. Shows data added after defense to show more data supported the claims in the thesis:

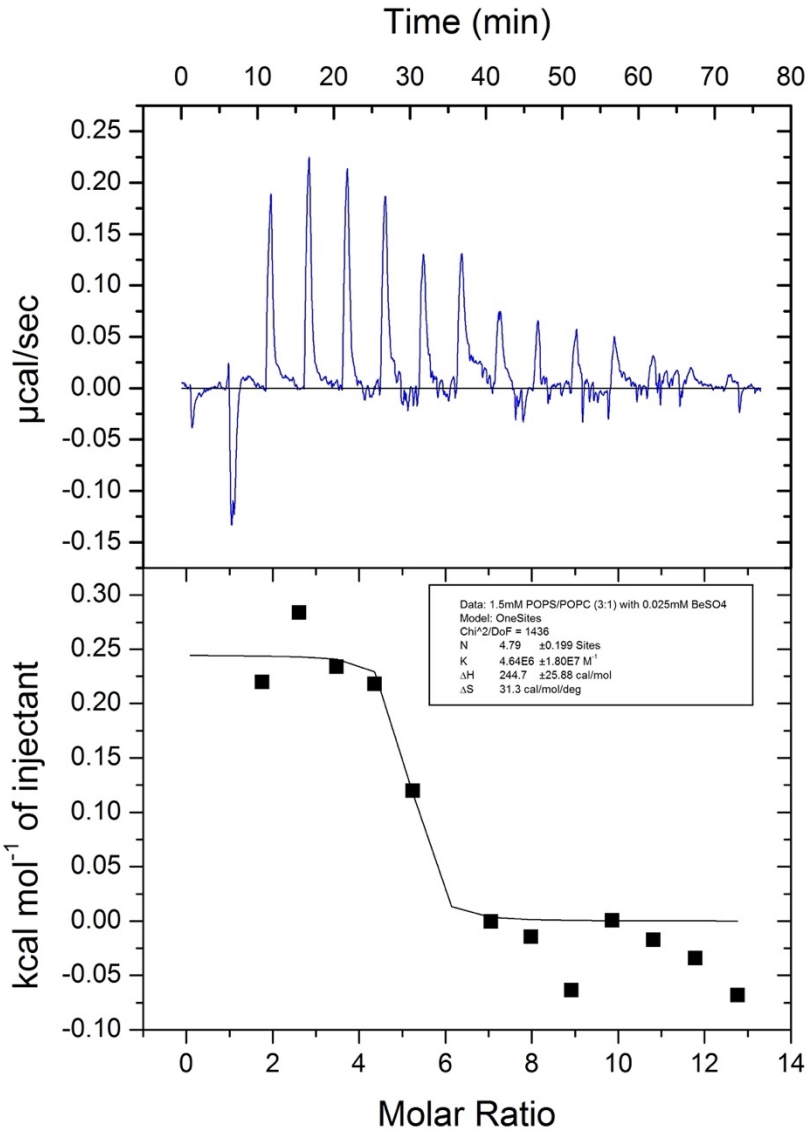

Fig SS 1. 1.5 mM POPS/POPC (3:1) with 25µM BeSO4 in 2mM Tris 10mM KCl

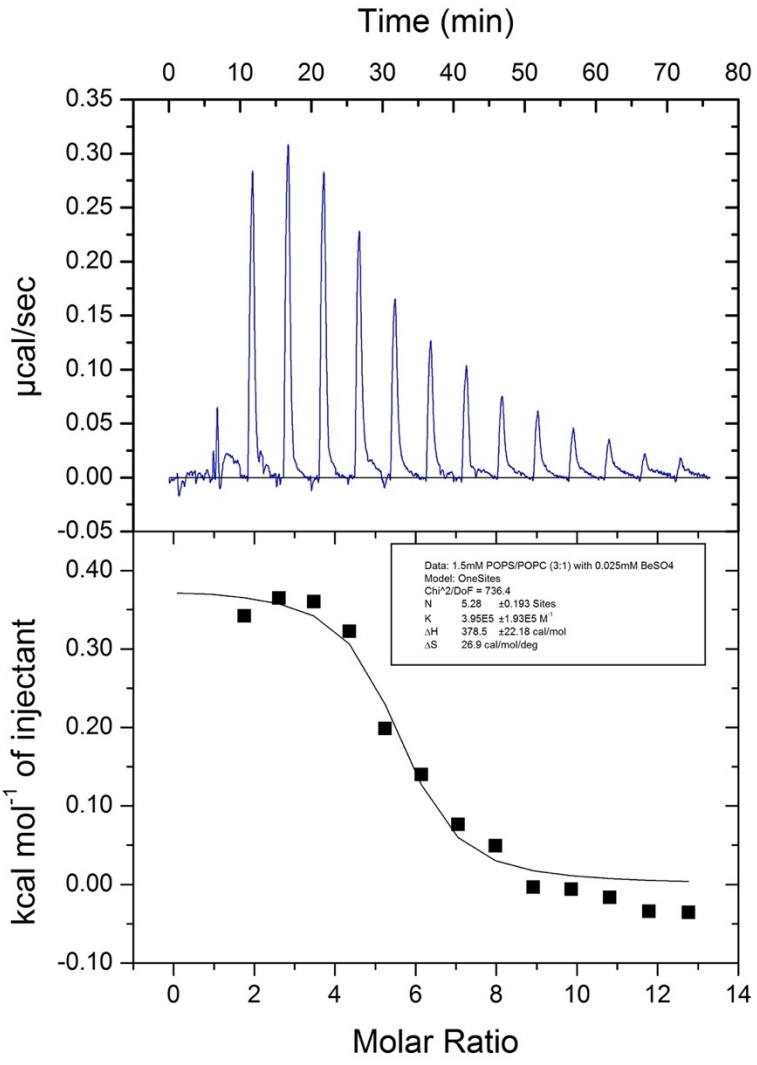

Fig SS 2. 1.5 mM POPS/POPC (3:1) with 25µM BeSO4 in 2mM Tris 10mM KCl

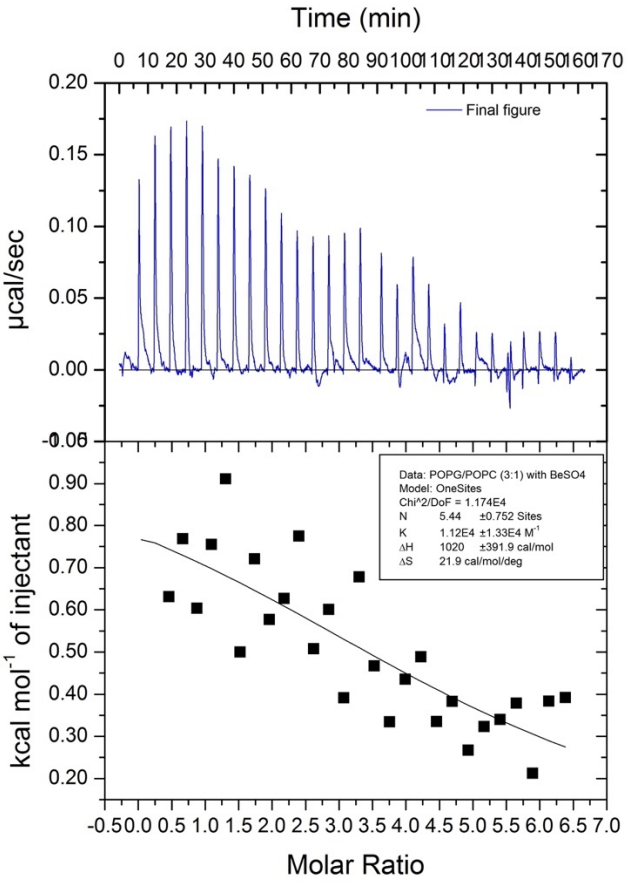

Fig SS 3. 1.5 mM POPG/POPC (3:1) with 50µM BeSO4 in 2mM Tris 10mM KCl

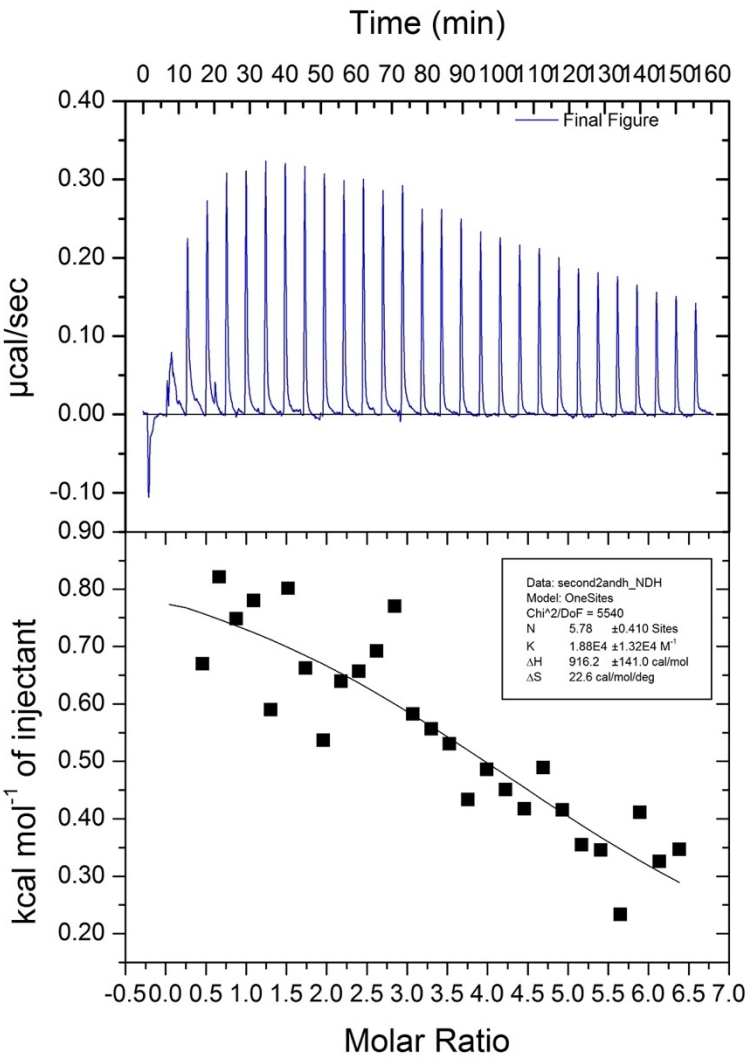

Fig SS 4. 1.5 mM POPG/POPC (3:1) with 50µM BeSO4 in 2mM Tris 10mM KCl

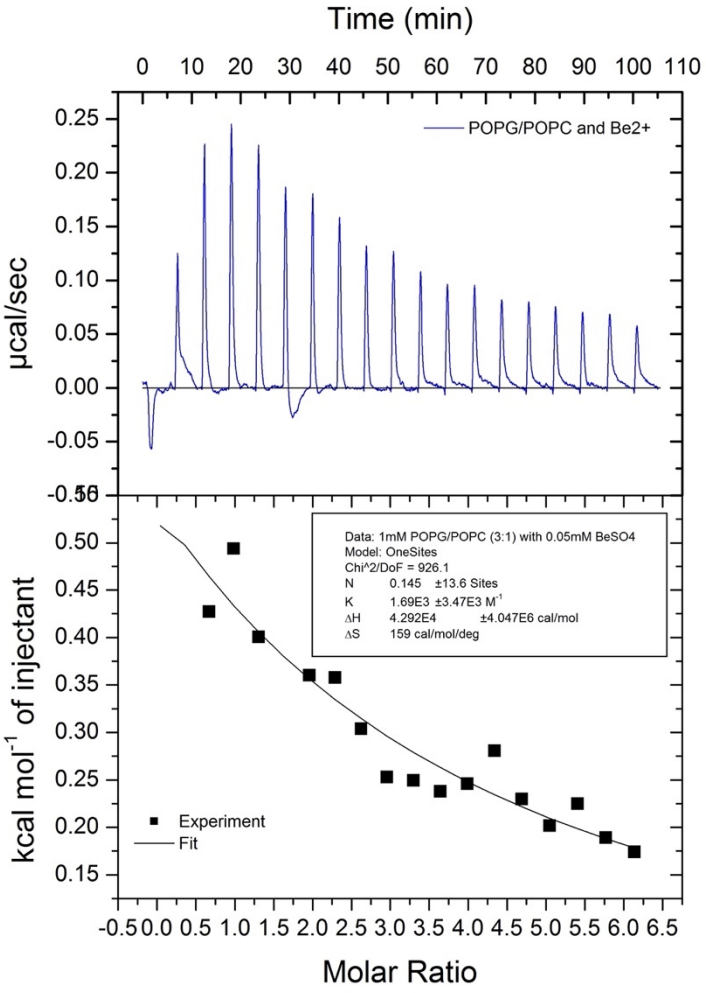

Fig SS 5. 1.5 mM POPG/POPC (3:1) with 50µM BeSO4 in 2mM Tris 10mM KCl

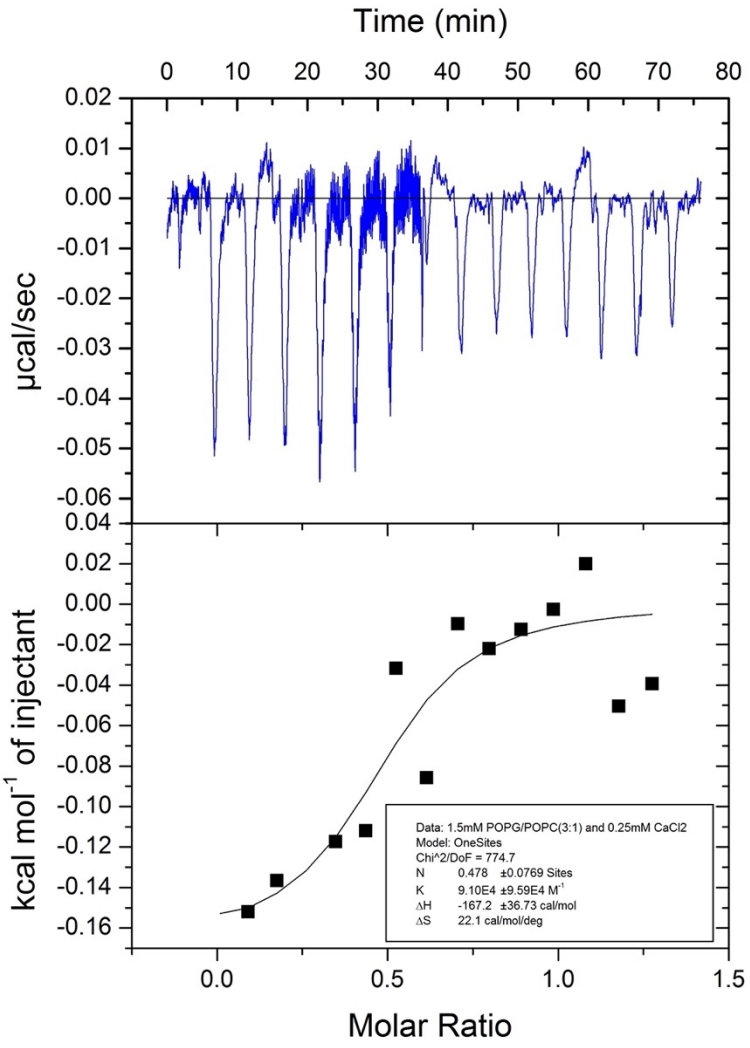

Fig SS 6. 1.5 mM POPG/POPC (3:1) with 250µM CaCl2 in 2mM Tris 10mM KCl

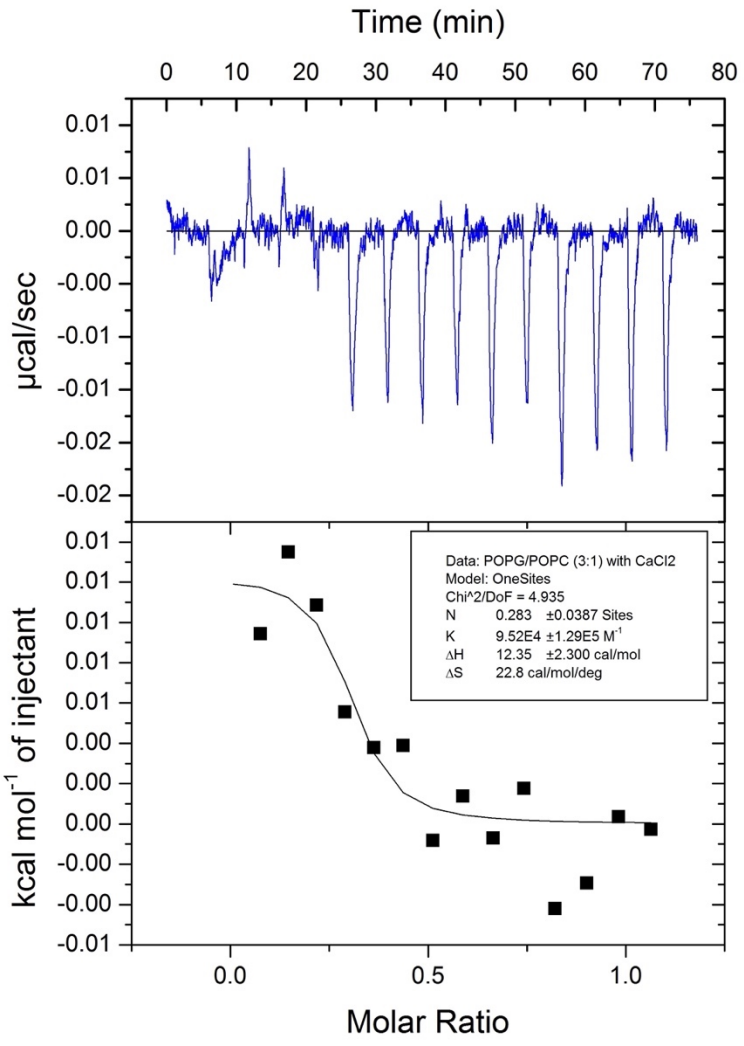

Fig SS 7. 5 mM POPG/POPC (3:1) with 1mM CaCl2 in 2mM Tris 10mM KCl

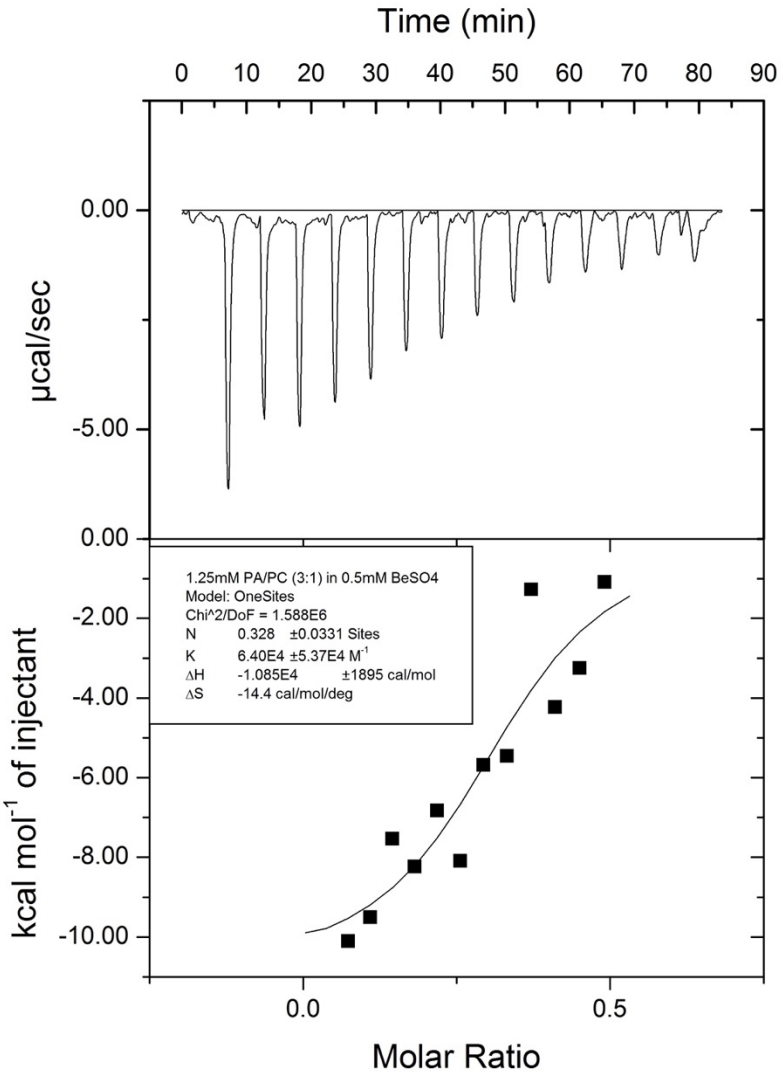

Fig SS 8. 1.25mM POPA//POPC in 0.5mM BeSO4 in 10 mM KCl 10 mM Tris

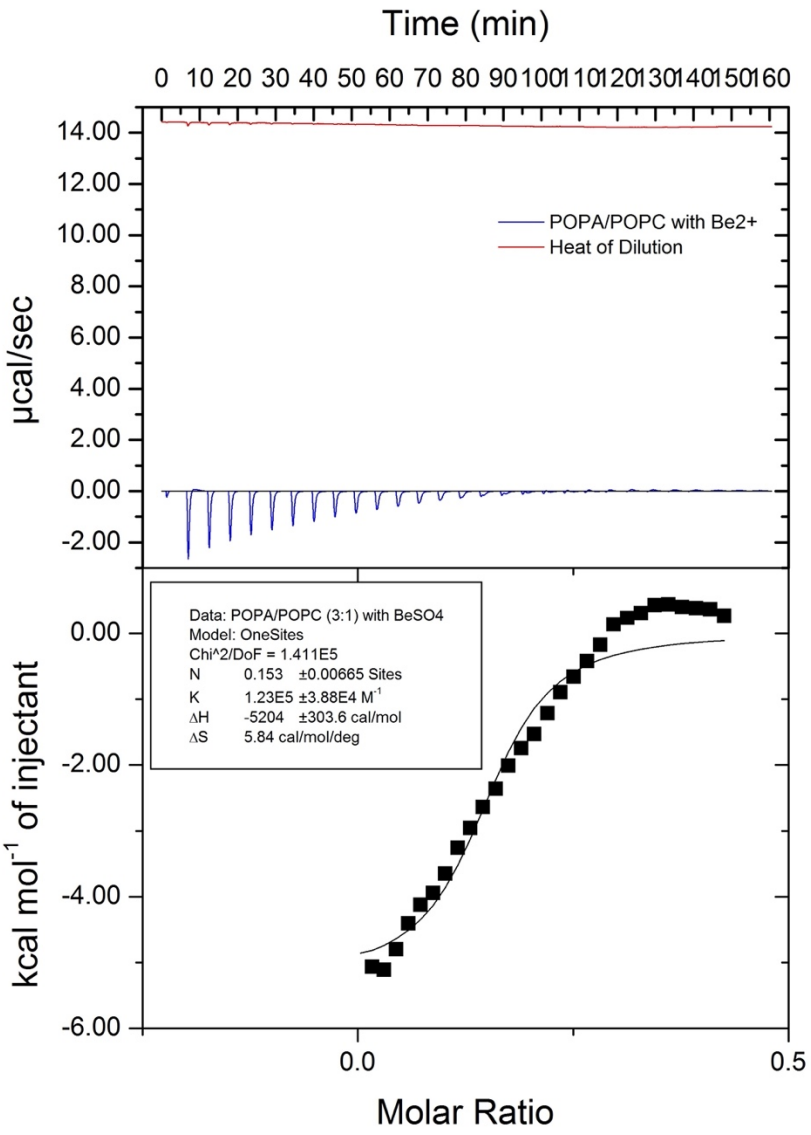

Fig SS 9. 1.5mM POPA//POPC in 0.25mM BeSO4 in 10 mM KCl 10 mM Tris

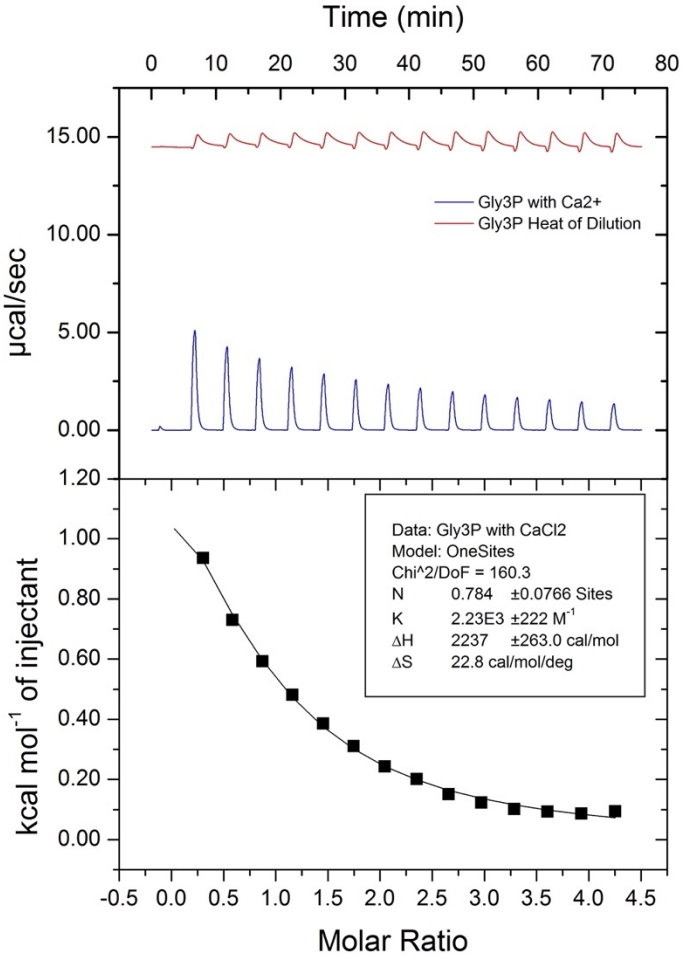

Fig SS 10. 10mM Gly3P and 0.5mM CaCl2 in 2mM Tris 10mM KCl

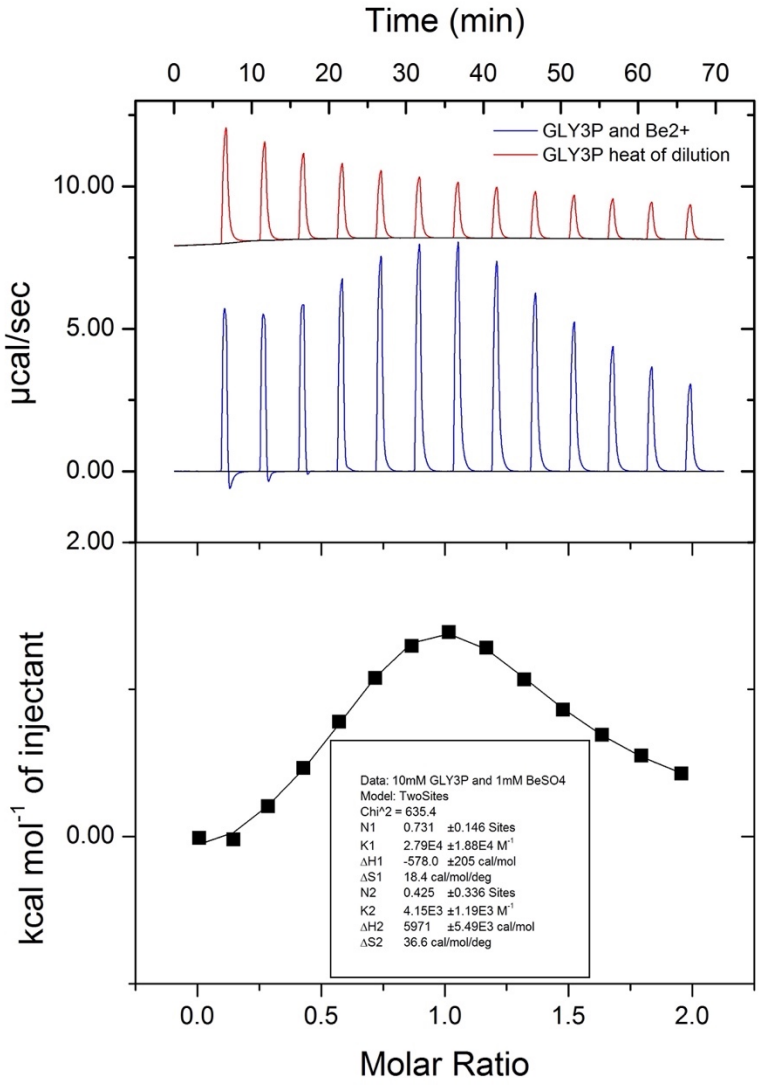

Fig SS 11. 10mM Gly3P and 0.5mM BeSO4 in 2mM Tris 10mM KCl

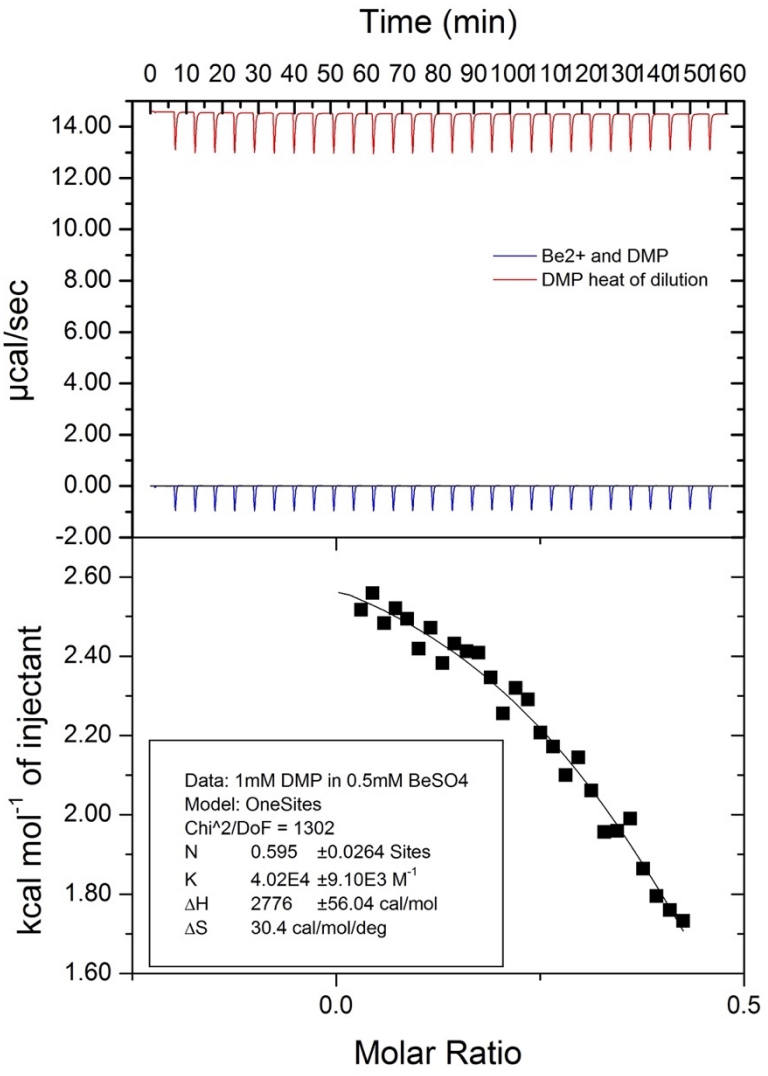

Fig SS 12. 1mM DMP and 0.5mM BeSO4 in 2mM Tris 10mM KCl

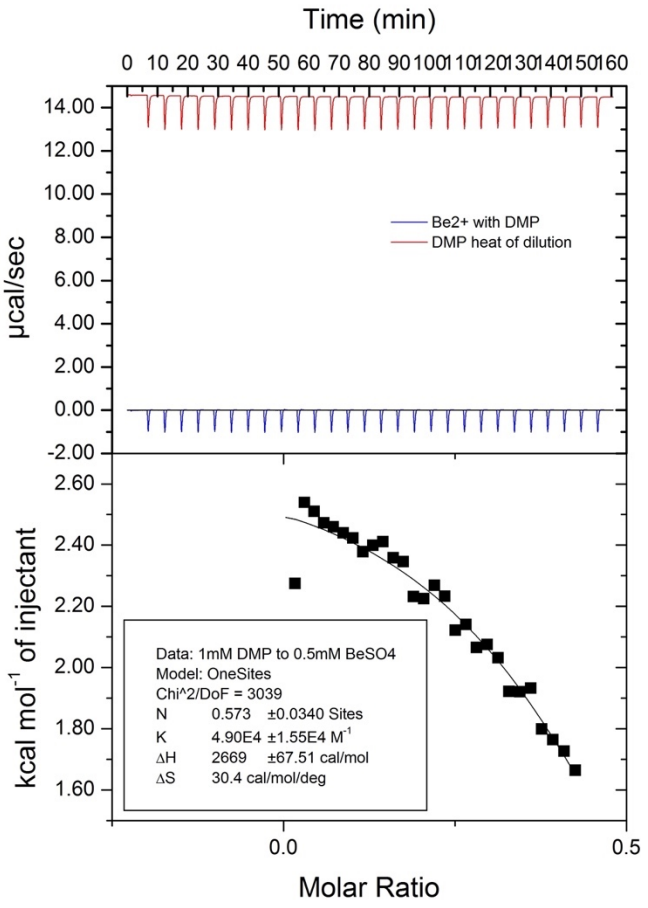

Fig SS 13. 1mM DMP and 0.5mM BeSO4 in 2mM Tris 10mM KCl

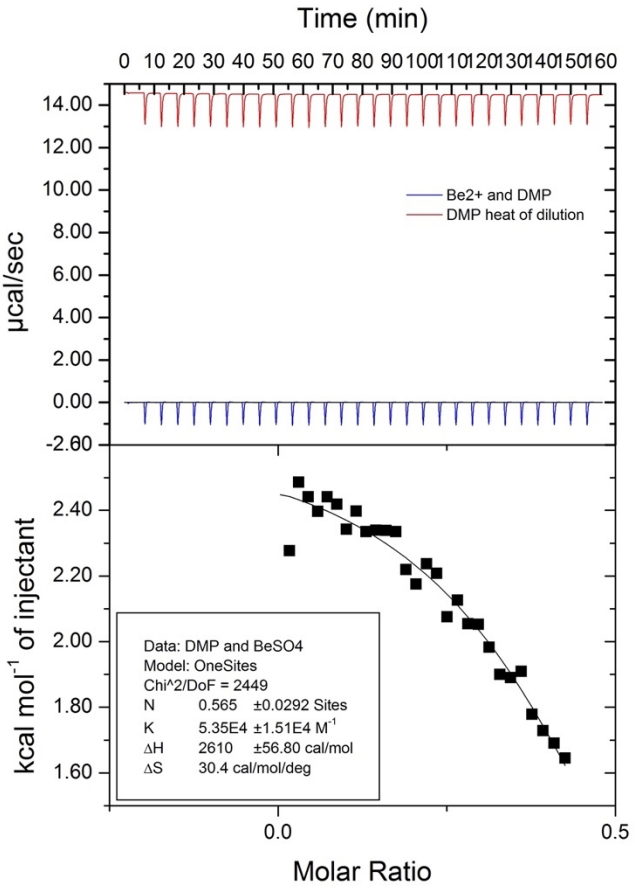

Fig SS 14. 1mM DMP and 0.5mM BeSO4 in 2mM Tris 10mM KCl

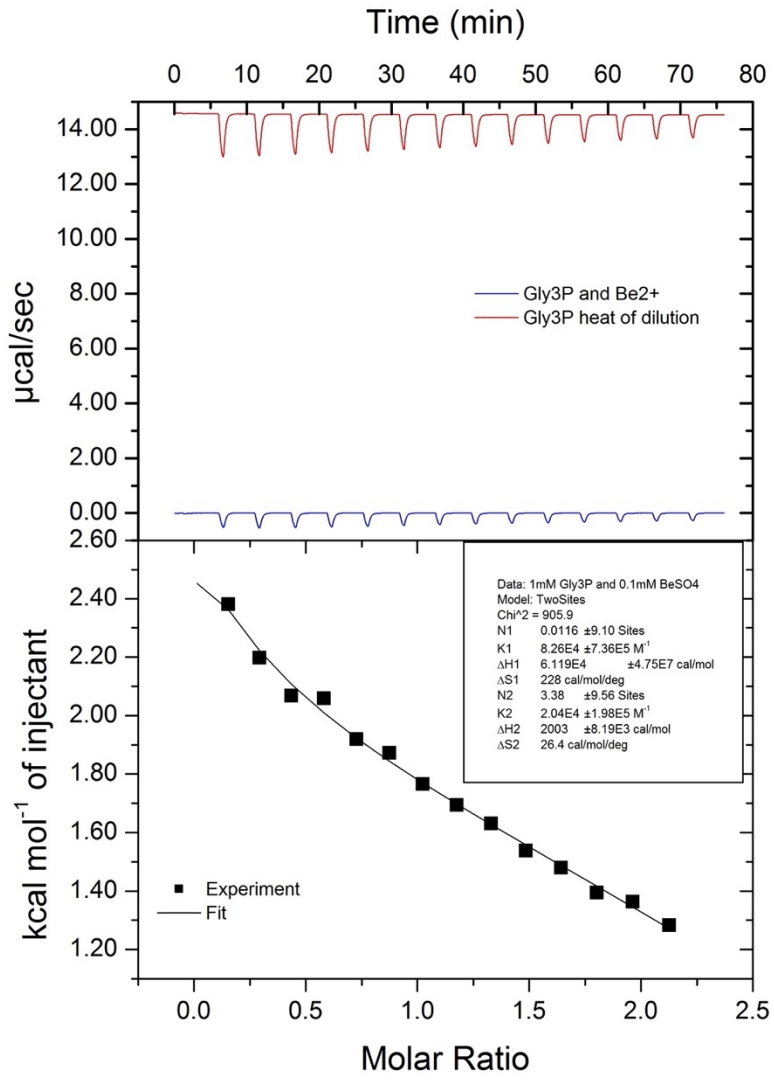

Fig SS 15. 0.1mM BeSO4 and 1mM Gly3P in 2mM Tris 10mM KCl pH not accurate but around 6

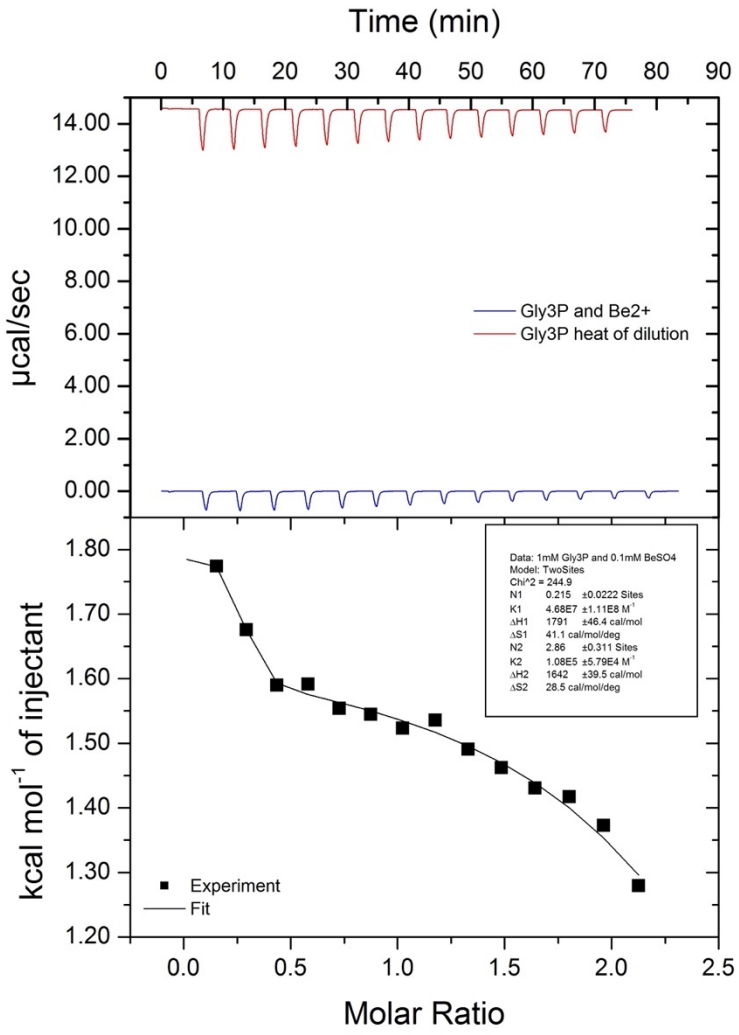

Fig SS 16. 0.1mM BeSO4 and 1mM Gly3P in 2mM Tris 10mM KCl pH not accurate but around 6

Bibliography

(1) Kolanz, M. E. Introduction to Beryllium: Uses, Regulatory History, and Disease. *Appl. Occup. Environ. Hyg.* **2001**, *16* (5), 559–567. https://doi.org/10.1080/10473220119088.

(2) Drobyshev, E.; Kybarskaya, L.; Dagaev, S.; Solovyev, N. New Insight in Beryllium Toxicity Excluding Exposure to Beryllium-Containing Dust: Accumulation Patterns, Target Organs, and Elimination. *Arch. Toxicol.* **2019**, *93* (4), 859–869. https://doi.org/10.1007/s00204-019-02432-7.

(3) Ermakov, Y. A.; Kamaraju, K.; Dunina-Barkovskaya, A.; Vishnyakova, K. S.; Yegorov, Y. E.; Anishkin, A.; Sukharev, S. High-Affinity Interactions of Beryllium(2+) with Phosphatidylserine Result in a Cross-Linking Effect Reducing Surface Recognition of the Lipid. *Biochemistry* **2017**, *56* (40), 5457–5470. https://doi.org/10.1021/acs.biochem.7b00644.

(4) Yoo, J.; Wilson, J.; Aksimentiev, A. Improved Model of Hydrated Calcium Ion for Molecular Dynamics Simulations Using Classical Biomolecular Force Fields. *Biopolymers* **2016**, *105* (10), 752–763. https://doi.org/10.1002/bip.22868.

(5) Leonard, A. N.; Klauda, J. B.; Sukharev, S. Isothermal Titration Calorimetry of Be^{2+} with Phosphatidylserine Models Guides All-Atom Force-Field Development for Lipid–Ion Interactions. *J. Phys. Chem. B* **2019**, *123* (7), 1554–1565. https://doi.org/10.1021/acs.jpcb.8b11884.

(6) Klasczyk, B.; Knecht, V. Validating Affinities for Ion–Lipid Association from Simulation against Experiment. *J. Phys. Chem. A* **2011**, *115* (38), 10587–10595. https://doi.org/10.1021/jp202928u.

(7) Redondo-Morata, L.; Giannotti, M. I.; Sanz, F. Structural Impact of Cations on Lipid Bilayer Models: Nanomechanical Properties by AFM-Force Spectroscopy. *Mol. Membr. Biol.* **2014**, *31* (1), 17–28. https://doi.org/10.3109/09687688.2013.868940.

(8) Böckmann, R. A.; Hac, A.; Heimburg, T.; Grubmüller, H. Effect of Sodium Chloride on a Lipid Bilayer. *Biophys. J.* **2003**, *85* (3), 1647–1655. https://doi.org/10.1016/S0006-3495(03)74594-9.

(9) Yang, H.; Xu, Y.; Gao, Z.; Mao, Y.; Du, Y.; Jiang, H. Effects of Na^{+}, K^{+}, and Ca^{2+} on the Structures of Anionic Lipid Bilayers and Biological Implication. *J. Phys. Chem. B* **2010**, *114* (50), 16978–16988. https://doi.org/10.1021/jp1091569.

(10) Altenbach, C.; Seelig, J. Calcium Binding to Phosphatidylcholine Bilayers as Studied by Deuterium Magnetic Resonance. Evidence for the Formation of a Calcium Complex with Two Phospholipid Molecules. *Biochemistry* **1984**, *23* (17), 3913–3920. https://doi.org/10.1021/bi00312a019.

(11) Lehrmann, R.; Seelig, J. Adsorption of Ca2+ and La3+ to Bilayer Membranes: Measurement of the Adsorption Enthalpy and Binding Constant with Titration Calorimetry.

Biochim. Biophys. Acta BBA - Biomembr. **1994**, *1189* (1), 89–95. https://doi.org/10.1016/0005-2736(94)90284-4.
(12) McCleskey, T. M.; Scott, B. L. Beryllium and Strong Hydrogen Bonds. *J. Occup. Environ. Hyg.* **2009**, *6* (12), 751–757. https://doi.org/10.1080/15459620903025574.
(13) Wiseman, T.; Williston, S.; Brandts, J. F.; Lin, L.-N. Rapid Measurement of Binding Constants and Heats of Binding Using a New Titration Calorimeter. *Anal. Biochem.* **1989**, *179* (1), 131–137. https://doi.org/10.1016/0003-2697(89)90213-3.
(14) Velazquez-Campoy, A. Geometric Features of the Wiseman Isotherm in Isothermal Titration Calorimetry. *J. Therm. Anal. Calorim.* **2015**, *122* (3), 1477–1483. https://doi.org/10.1007/s10973-015-4775-x.
(15) *CRC Handbook of Chemistry and Physics: A Ready-Reference Book of Chemical and Physical Data*, 76. ed., 1995–1996.; Lide, D. R., Chemical Rubber Company, Eds.; CRC Press: Boca Raton, Fla., 1995.
(16) Wang, X.; Devaiah, S.; Zhang, W.; Welti, R. Signaling Functions of Phosphatidic Acid. *Prog. Lipid Res.* **2006**, *45* (3), 250–278. https://doi.org/10.1016/j.plipres.2006.01.005.